



Review

Basic Aspects of Ferroelectricity Induced by Noncollinear Alignment of Spins

I. V. Solovyev

Research Center for Materials Nanoarchitectonics (MANA), National Institute for Materials Science (NIMS),
1-1 Namiki, Tsukuba 305-0044, Ibaraki, Japan; solovyev.igor@nims.go.jp

Abstract: Basic principles of ferroelectric activity induced by the noncollinear alignment of spins are reviewed. There is a fundamental reason why the inversion symmetry can be broken by certain magnetic order. This situation occurs when the magnetic order simultaneously involves ferromagnetic (F) and antiferromagnetic (A) counterparts, transforming under the spatial inversion \mathcal{I} and time reversal \mathcal{T} as $\mathcal{I}F = F$ and $\mathcal{I}\mathcal{T}A = A$, respectively. The incompatibility of these two conditions results in breaking the inversion symmetry, which manifests itself in the electric polarization \vec{P} . The noncollinear alignment of spins is one of examples of such coexistence of F and A . This coexistence principle imposes a constraint on possible dependencies of \vec{P} on the directions of spins, which can include only “antisymmetric coupling” in the bond, $\vec{P}_{ij} \cdot [e_i \times e_j]$, and “single-ion anisotropy”, $e_i \cdot \vec{P}_{ij} e_i$. Microscopically, \vec{P}_{ij} can be evaluated in the framework of superexchange theory. For the single Kramers doublet, this theory yields $\vec{P}_{ij} \sim \vec{r}_{ij}$, where \vec{r}_{ij} is the spin-dependent part of the position operator induced by the relativistic spin-orbit coupling. \vec{r}_{ij} remains invariant under spatial inversion, providing the microscopic reason why noncollinear alignment of spins can induce \vec{P} even in centrosymmetric crystals. The symmetry properties of \vec{r}_{ij} can be rationalized from the viewpoint of symmetry of Kramers states. Particularly, the commonly used Katsura–Nagaosa–Balatsky (KNB) rule $\vec{P} \propto \vec{\epsilon}_{ji} \times [e_i \times e_j]$ ($\vec{\epsilon}_{ji}$ being the direction of the bond ij) can be justified only for relatively high symmetry of the bonds. The single-ion anisotropy vanishes for the spin $\frac{1}{2}$ or if magnetic ions are located in inversion centers, thus severely restricting the applicability of this microscopic mechanism. The properties of multiferroic materials are reconsidered from the viewpoint of these principles. A particular attention is paid to complications caused by possible deviations from the KNB rule.



Academic Editor: Naurang L. Saini

Received: 11 March 2025

Revised: 8 April 2025

Accepted: 9 April 2025

Published: 11 April 2025

Citation: Solovyev, I.V. Basic Aspects of Ferroelectricity Induced by Noncollinear Alignment of Spins. *Condens. Matter* **2025**, *10*, 21. <https://doi.org/10.3390/condmat10020021>

Copyright: © 2025 by the author. Licensee MDPI, Basel, Switzerland. This article is an open access article distributed under the terms and conditions of the Creative Commons Attribution (CC BY) license (<https://creativecommons.org/licenses/by/4.0/>).

Keywords: multiferroics; Mott insulators; noncollinear magnets; electric polarization; magnetoelectric effect; spin-orbit coupling; Wannier function methods

1. Introduction

The ferroelectricity is the property of insulating materials to possess spontaneous electric polarization \vec{P} [1]. Since the spatial inversion operation \mathcal{I} changes the sign of \vec{P} , it is essential that \mathcal{I} must be broken. In this sense, the search of new ferroelectric materials is basically the search of new mechanisms of breaking the inversion symmetry and possibilities to realize these mechanisms in practice.

Canonically, the inversion symmetry breaking is associated with the properties of nonmagnetic crystalline lattice, whose atomic positions do not transform to themselves by \mathcal{I} . Here, the polar distortion induces the additional mixing between occupied bonding and unoccupied antibonding states and, if this mixing lowers the energy, the distortion

becomes stable [2,3]. The typical mechanism promoting such mixing is the transition metal $3d$ - oxygen $2p$ hybridization in d^0 perovskite oxides like PbTiO_3 and BaTiO_3 [3].

A very special case of ferroelectricity is when \mathcal{I} is broken by a magnetic alignment of spins. From the canonical point of view, the idea may look rather counterintuitive, because the magnetism is typically associated with breaking time reversal symmetry \mathcal{T} , while breaking \mathcal{I} was believed to be the prerogative of atomic displacements [4]. Nevertheless, such a possibility was predicted in 1960 by Dzyaloshinskii [5]. He realized that the magnetic structure of some antiferromagnetic (AFM) materials, such as Cr_2O_3 , can be transformed to itself by combining \mathcal{I} with \mathcal{T} . Therefore, both \mathcal{I} and \mathcal{T} can be simultaneously broken by applying a magnetic field \mathbf{H} , which will induce not only the net magnetization, but also the electric polarization \vec{P} . Such materials are now called magnetoelectrics. The key point here is that \mathbf{H} deforms the AFM alignment of spins and make it noncollinear, which is crucial for breaking the inversion symmetry. Therefore, the next step was to realize the same effect but without external magnetic field, by exploiting for these purposes the intrinsic noncollinearity of spin-spiral magnets arising from competition between several exchange interactions operating in different bonds. The materials, where the inversion symmetry is spontaneously broken by intrinsic magnetic order without external magnetic field are called type-II multiferroics. We do not consider here type-I multiferroics, where the ferroelectricity and ferromagnetism have a different origin and can exist independently on each other [4,6]. Therefore, “multiferroics” in this review will solely mean type-II multiferroics. This direction became extremely popular in early 2000s, after the discovery of ferroelectric activity in the spin-spiral magnet TbMnO_3 [7] and other materials [8], and still attracts a lot of attention today as it provides a unique possibility for the cross-control of magnetization and polarization by electric and magnetic fields [9,10]. Nevertheless, it is worth to remark that although the primary emphasize was given to the search of spin-spiral multiferroics [8,11], historically they were not the first multiferroics. For instance, the inversion symmetry breaking arising from incompatibility of magnetic orders in the rare-earth (R) and transition-metal (M) sublattices was predicted in orthorhombically distorted perovskites RMO_3 as early as in 1973 [12].

The modern theory of electric polarization was developed by King-Smith and Vanderbilt in early 1990s [13,14]. It has two equivalent formulations: in the reciprocal space, in terms of the Berry connection, and in the real space, in terms of the Wannier functions $|w_i\rangle$ for the occupied bands. The latter formulation is more convenient for the construction of microscopic models, using for these purposes the perturbation theory in the real space. It states that the electric polarization \vec{P} (actually, the change of polarization in the process of adiabatic lowering the symmetry) is given by expectation values of the position operator \vec{r} in the basis of these Wannier functions as

$$\vec{P} = -\frac{e}{V} \sum_i \langle w_i | \vec{r} | w_i \rangle, \quad (1)$$

where $-e$ is the electron charge, V is the volume, and i is the lattice point (the Wannier center) [13–15]. This theory was spurred by growing interest in ferroelectric materials as well as the phenomenon of ferroelectricity itself and provided a long-awaited solution of the problem on how to properly calculate \vec{P} in periodic systems, especially in first-principles electronic structure methods. It was still one decade before the new era of multiferroics, sparked in early 2000s, and no consideration of magnetic dependencies of electric polarization was given around that time. Nevertheless, the idea seems to be straightforward: since \vec{r} does not depend on magnetic degrees of freedom, all information about the magnetism is included in $|w_i\rangle$ and what we have to do is to understand how $|w_i\rangle$ evolves with the change of magnetic structures.

The Katsura-Nagaosa-Balatsky (KNB) rule for electric polarization induced by spiral magnetic order was formulated in 2005 [16], soon after discovery of this effect in TbMnO₃ [7]. It relates the direction of polarization in the bond with the ones of magnetic moments e_1 and e_2 as $\vec{P} \propto \vec{e}_{21} \times [e_1 \times e_2]$, where \vec{e}_{21} is the direction of the bond. The rule appeared to be rather universal and readily explained the main trends in the behavior of quite a large number of multiferroic materials with spiral magnetic order [6,8,11,17].

The KNB theory, being the first microscopic theory of magnetoelectric coupling and explaining the appearance of electric polarization in noncollinear magnets, played a very important role in understanding the properties of multiferroic materials and the phenomenon of multiferroicity itself. However, there are also many concerns about universality, validity, and generality of the KNB rule. In their original work, KNB considered a very simple and very special model for the centrosymmetric bond, in which the magnetic d states at the edges were mediated by the ligand p states in the midpoint of the bond. The magnetic states were also taken in the very special form of twofold degenerate Γ_7 representation formed by cubic xy , yz , and zx orbitals in the presence of relativistic spin-orbit (SO) coupling. Thus, it is not clear to which extend the expression for the electric polarization, derived for this special case, can be and should be applied for the analysis of magnetoelectric coupling in all types of multiferroic materials, as it is typically done today. Moreover, despite a formal simplicity, the KNB model does not provide a clear answer why the noncollinear magnetic order breaks the inversion symmetry and which microscopic invariant is responsible for finite polarization in centrosymmetric crystals.

The situation was further complicated by discoveries of new multiferroic materials, where the electric polarization is induced by proper screw magnetic order with the spins rotating in the plane perpendicular to the bonds, i.e., where the canonical KNB theory predicts no electric polarization [18–20]. This has led to the proposal of yet another popular mechanism of magnetically induced ferroelectricity, the so-called spin-dependent metal-ligand hybridization mechanism [18], which is regarded as supplementary to the KNB one [17]. However, even though the conventional KNB picture may look at odds with the properties of certain multiferroic materials, is it because of additional simplifications considered by KNB (while the basic idea itself is still vital) or does it mean that this mechanism cannot work in principle and one has to consider alternative possibilities?

The goal of this review article is to explain, from the very basic point of view, why and how the electric polarization can be induced by the noncollinear alignment of spins. We start with simple phenomenological considerations and argue why the noncollinear alignment of spins breaks the inversion symmetry. This phenomenological picture will help us to understand how the electric polarization should depend on the relative directions of spins. Particularly, for the centrosymmetric bond, there can be only two contributions to \vec{P} : in the form of the antisymmetric exchange coupling and single-ion anisotropy.

Then, we turn to a microscopic picture for the magnetically dependent polarization. Formally, the derivation of KNB does not rely on modern theory of electric polarization. However, the perturbation theory considered by KNB can be viewed as a particular way to evaluate Wannier functions $|w_i\rangle$ for the occupied states, which is required by the modern theory. We will explain how this can be done rigorously by considering the superexchange-type theory for electric polarization. This theory will give us a clear answer which microscopic parameter is responsible for the magnetoelectric coupling in centrosymmetric materials. The form of the coupling between noncollinear spins and the electric polarization can be more general than the one prescribed by the KNB rule. The latter can be recovered only for threefold rotational or higher symmetries of the bond. Furthermore, we will rationalize the behavior of the single-ion anisotropy for the electric polarization and argue that this contribution should vanish at least in the following two cases: for

the spin $\frac{1}{2}$ and if the magnetic ion is located in the centrosymmetric position. Since the spin-dependent metal-ligand hybridization is one of the microscopic mechanism for the single-ion anisotropy, our finding severely restricts its applicability. With this in mind, we will reconsider the behavior of known multiferroic materials and the roles played by different microscopic mechanisms in this behavior.

2. Reasons of Inversion Symmetry Breaking

Consider a bond connecting the sites 1 and 2 with the inversion center in the midpoint (Figure 1). Let e_1 and e_2 be the directions of spins at the sites 1 and 2, which are normalized to unity. Then, any noncollinear alignment of spins e_1 and e_2 can be viewed as a superposition of ferromagnetic (FM) and AFM order parameters, which are given by $F = e_1 + e_2$ and $A = e_1 - e_2$, respectively. F has the symmetry of the bond and is transformed to itself by the spatial inversion about the midpoint: $\mathcal{I}F = F$. However, in order to keep A invariant, it is essential to combine \mathcal{I} with \mathcal{T} , which additionally transforms each e_i to $-e_i$ ($i = 1$ or 2), yielding $\mathcal{I}\mathcal{T}A = A$.

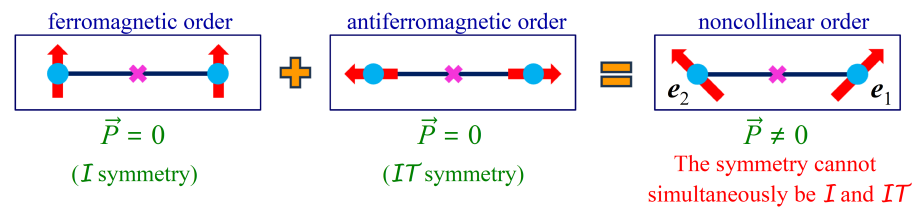


Figure 1. Cartoon picture explaining inversion symmetry breaking by noncollinear magnetic alignment in otherwise centrosymmetric bond. The crystallographic inversion center is denoted by \times . The ferromagnetic order (F) is invariant under the spatial inversion \mathcal{I} . The antiferromagnetic order (A) is invariant under the symmetry operation $\mathcal{I}\mathcal{T}$, where \mathcal{I} is combined with the time reversal \mathcal{T} . In both cases, the electric polarization \vec{P} is equal to zero. The noncollinear order can be viewed as a superposition of the collinear orders F and A . Since the \mathcal{I} and $\mathcal{I}\mathcal{T}$ symmetries (required by, respectively, F and A counterparts) cannot coexist, the inversion symmetry is broken, resulting in finite \vec{P} . e_1 and e_2 are the directions of spins at two sites of the bonds.

Thus, although inversion symmetry can be preserved separately for the F or A order (either alone or in the combination with \mathcal{T}), it appears to be broken in the case of noncollinear alignment of spins, where both order parameters are finite: simply, there is no such symmetry operation, which would simultaneously transform F and A to themselves. Hence, the system can develop finite polarization \vec{P} . The explanation is general and equally apply to the canonical magnetoelectric effect in antiferromagnetic Cr_2O_3 [5], where the noncollinearity of spins is induced by H , destroying the $\mathcal{I}\mathcal{T}$ symmetry of AFM alignment, or multiferroics, where this noncollinearity stems from competition of isotropic exchange interactions [16]. In this sense, the multiferroic can be viewed as an intrinsic magnetoelectric, in which the internal field due to F plays the role of H .

In the notations here and elsewhere in the paper, the vector symbol is reserved for the direction of electric polarization \vec{P} and related to it quantities such as the position operator \vec{r} and electric field \vec{E} , while other vector quantities, related to magnetic degrees of freedom, are denoted by bold symbols.

3. Spin Dependence of Induced Polarization: A Phenomenological View

In the previous section, we have seen that in order to break the inversion symmetry by magnetic means, the ferromagnetic order parameter in the centrosymmetric bond, F , should coexist with the antiferromagnetic one, A , meaning that the spins in the bond are noncollinear to each other. Therefore, the induced polarization \vec{P} should be proportional to both F and A . The most general combination of F and A is the 3×3 matrix $F^T \otimes A$

of Kronecker product, where F^T is the row-vector, corresponding to the column-vector F . Then, it is straightforward to find that (see Supplementary Material):

$$\vec{P} = \vec{\mathcal{P}}_{12} \cdot [e_1 \times e_2] + e_1 \cdot \overset{\circ}{\mathbb{T}} e_1 - e_2 \cdot \overset{\circ}{\mathbb{T}} e_2. \quad (2)$$

Thus, there can be only two source of polarization in centrosymmetric bonds. The first one is the antisymmetric coupling, which is proportional to the cross product of e_1 and e_2 , similar to antisymmetric Dzyaloshinskii-Moriya (DM) interaction $D_{12} \cdot [e_1 \times e_2]$ [21,22]. Nevertheless, $D_{12} = [D_{12}^c]$ is a vector, while $\vec{\mathcal{P}}_{12} = [\mathcal{P}_{12}^{v,c}]$ is the rank-2 tensor, where the first index (v) is reserved for the vector component of electric polarization and the second index (c) stands to describe the coupling with the spin vector, which is given by the cross product $[e_1 \times e_2]$. Furthermore, D_{12} vanishes in the centrosymmetric bond, while $\vec{\mathcal{P}}_{12}$ does not. The second source is the single-ion anisotropy, described by the rank-3 tensor $\overset{\circ}{\mathbb{T}} = [\overset{\circ}{\mathbb{T}}^{v,ab}]$ (where v is referred to the direction of electric polarization, while a and b describe the coupling with spins). If the bond is centrosymmetric, the single-ion contribution is finite only when $e_2 \neq e_1$ (i.e., the spins are noncollinear).

No other contributions to \vec{P} except these two are expected. For instance, there should be no symmetric (with respect to the permutation of e_1 and e_2) contributions to \vec{P} , neither isotropic nor anisotropic ones. If 1 and 2 are the edges of isolated dimer, the tensor $\overset{\circ}{\mathbb{T}}$ is finite (except for the special case of $S = \frac{1}{2}$ [23], which will be considered in Section 6). Nevertheless, if the bond is a part of the solid, it is quite common that the atoms forming the bond are located in inversion centers. Then, $\overset{\circ}{\mathbb{T}}$ should vanish.

Being in line with these phenomenological considerations, most of microscopic models, so far proposed for the analysis of magnetoelectric coupling in noncollinear magnets, were focusing on either the antisymmetric exchange in magnetic bonds [16,24] or the single-ion anisotropy [18,25]. Other forms of magnetic dependence of the electric polarization in noncollinear magnets would be exotic, at least from this phenomenological point of view.

4. Microscopic Picture

The simplest microscopic expression for $\vec{\mathcal{P}}_{12}$ can be derived by considering the following chain arguments [26]. Since the electric polarization in metals is screened by free electrons, the ferroelectricity is the property of insulating materials. Then, vast majority of magnetic insulators are Mott insulators, where both magnetism and insulating behavior are due to the large on-site Coulomb repulsion U . Therefore, it is natural to assume that magnetic ferroelectrics (or multiferroics) belong to the same category. The key theory for interatomic exchange interactions in Mott insulators is Anderson's superexchange (SE) theory [27]. It starts with the limit of large U and in each bond (ij) treats electronic hoppings \hat{t}_{ij} as a perturbation. Basically, the SE theory is the second order perturbation theory for the energy with respect to \hat{t}_{ij} . Our goal is to formulate a similar theory for the polarization \vec{P} given by Equation (1). Since the position operator itself does not depend on spin, the magnetoelectric coupling arises entirely from the spin dependence of the Wannier functions. Then, the first observation is that, instead of the second order perturbation theory for the energy, the SE theory can be formulated by considering the first order perturbation theory for $|w_i\rangle$. Indeed, if $|w_i\rangle = |\alpha_i^o\rangle$ is the occupied atomic state in the limit $U \rightarrow \infty$, the electronic hoppings will induce a tail spreading to the neighboring site j :

$$|w_i\rangle \approx |\alpha_i^o\rangle + |\alpha_{i \rightarrow j}^o\rangle. \quad (3)$$

To the first order in \hat{t}_{ji}/U , this tail is given by:

$$|\alpha_{i \rightarrow j}^o\rangle = -\frac{1}{U} |\alpha_j^u\rangle \langle \alpha_j^u | \hat{t}_{ji} | \alpha_i^o\rangle, \quad (4)$$

where $|\alpha_j^u\rangle$ is the unoccupied state in the atomic limit. Then, using Equations (3) and (4), it is straightforward to evaluate the energy change caused by \hat{t}_{ij} . For the dimer in Figure 1, it is given by:

$$\mathcal{E} = -\frac{2|\langle\alpha_1^o|\hat{t}_{12}|\alpha_2^u\rangle|^2}{U}, \tag{5}$$

which is totally consistent with the well-known expression in the SE theory [27]. Nevertheless, the advantage of using the perturbation theory for the Wannier function is that it can be directly applied to the polarization (1), which can be now expressed via combinations of $\langle\alpha_1^o|\hat{t}_{12}|\alpha_2^u\rangle$ with similar matrix elements of \vec{r} between occupied and unoccupied states at the sites 1 and 2 [26]:

$$\begin{aligned} \vec{P} = \frac{e}{VU} \{ & \langle\alpha_1^o|\hat{r}_{12}|\alpha_2^u\rangle\langle\alpha_2^u|\hat{t}_{21}|\alpha_1^o\rangle + \langle\alpha_1^o|\hat{t}_{12}|\alpha_2^u\rangle\langle\alpha_2^u|\hat{r}_{21}|\alpha_1^o\rangle \\ & + \langle\alpha_2^o|\hat{r}_{21}|\alpha_1^u\rangle\langle\alpha_1^u|\hat{t}_{12}|\alpha_2^o\rangle + \langle\alpha_2^o|\hat{t}_{21}|\alpha_1^u\rangle\langle\alpha_1^u|\hat{r}_{12}|\alpha_2^o\rangle \}. \end{aligned} \tag{6}$$

Then, we need to specify the o and u states and relate them to the direction of spin (or pseudospin). Suppose, there is some basis of Kramers states, $|+\rangle$ and $|-\rangle$, so that \hat{t}_{12} and \hat{r}_{12} in Equation (6) are the matrices in the basis of these states. Then, one can choose:

$$|\alpha_i^o\rangle = \cos\frac{\theta_i}{2}|i+\rangle + \sin\frac{\theta_i}{2}e^{i\phi_i}|i-\rangle, \tag{7}$$

such that $\langle\alpha_i^o|\hat{\sigma}|\alpha_i^o\rangle = (\sin\theta_i\cos\phi_i, \sin\theta_i\sin\phi_i, \cos\theta_i) \equiv \mathbf{e}_i$ is the direction of spin at the site i and $\hat{\sigma} = (\hat{\sigma}^x, \hat{\sigma}^y, \hat{\sigma}^z)$ is the vector of Pauli matrices, where $|+\rangle$ and $|-\rangle$ are the eigenstates of $\hat{\sigma}_z$: $\hat{\sigma}_z|+\rangle = |+\rangle$ and $\hat{\sigma}_z|-\rangle = -|-\rangle$. The u state can be chosen as:

$$|\alpha_i^u\rangle = -\sin\frac{\theta_i}{2}e^{-i\phi_i}|i+\rangle + \cos\frac{\theta_i}{2}|i-\rangle. \tag{8}$$

Then, \hat{t}_{12} and \hat{r}_{12} in Equation (6) can be decomposed in terms of the 2×2 unity matrix $\hat{\mathbb{1}}$ and the vector $\hat{\sigma}$ of Pauli matrices as $\hat{t}_{12} = t_{12}^0\hat{\mathbb{1}} + i\mathbf{t}_{12}\hat{\sigma}$ and $\hat{r}_{12} = \vec{r}_{12}^0\hat{\mathbb{1}} + i\vec{r}_{12}\hat{\sigma}$ with the real coefficients $(t_{12}^0, \mathbf{t}_{12})$ and $(\vec{r}_{12}^0, \vec{r}_{12})$. Strictly speaking, the consideration of a single Kramers doublet corresponds to the spin $S = \frac{1}{2}$. Nevertheless, the main conclusions are believed to be more general [16].

Substituting \hat{t}_{12} and \hat{r}_{12} in Equation (6) and using the explicit form of the o and u states, given by Equations (7) and (8), the magnetic part of the exchange energy and polarization can be presented in the form of bilinear interactions between \mathbf{e}_1 and \mathbf{e}_2 , which can be further decomposed into isotropic, antisymmetric, and traceless symmetric anisotropic parts as [26]:

$$\mathcal{E} = -J_{12}\mathbf{e}_1 \cdot \mathbf{e}_2 + \mathbf{D}_{12} \cdot [\mathbf{e}_1 \times \mathbf{e}_2] + \mathbf{e}_1 \cdot \mathbb{T}_{12}\mathbf{e}_2 \tag{9}$$

and

$$\vec{P} = \vec{P}_{12}\mathbf{e}_1 \cdot \mathbf{e}_2 + \vec{\mathcal{P}}_{12} \cdot [\mathbf{e}_1 \times \mathbf{e}_2] + \mathbf{e}_1 \cdot \vec{\mathbb{I}}_{12}\mathbf{e}_2. \tag{10}$$

Here, we use the following conventions: the bold roman letters, \mathbf{D}_{12} and $\vec{\mathcal{P}}_{12}$, stand for the vectors forming the scalar product with the spin vector $[\mathbf{e}_1 \times \mathbf{e}_2]$; the hollow symbols, \mathbb{T}_{12} and $\vec{\mathbb{I}}_{12}$, stand for the 3×3 tensors, acting on \mathbf{e}_1 from the left and \mathbf{e}_2 from the right. The additional vector sign in the case of \vec{P}_{12} , $\vec{\mathcal{P}}_{12}$, and $\vec{\mathbb{I}}_{12}$ denotes the direction of polarization.

The corresponding parameters are summarized in Table 1 [26].

Table 1. Isotropic (J_{12} and \vec{P}_{12}), antisymmetric (D_{12} and $\vec{\mathcal{P}}_{12}$), and traceless anisotropic symmetric (\mathbb{T}_{12} and $\vec{\mathbb{T}}_{12}$) parameters of exchange interactions and electric polarization. Tr denotes trace and $\mathbb{1}$ is the 3×3 unity matrix.

Exchange Interactions	Electric Polarization
$J_{12} = -\frac{(t_{12}^0)^2}{U}$	$\vec{P}_{12} = -\frac{2e}{V} \frac{\vec{r}_{12}^0 t_{12}^0}{U}$
$D_{12} = \frac{2t_{12}^0 \mathbf{t}_{12}}{U}$	$\vec{\mathcal{P}}_{12} = -\frac{2e}{V} \frac{\vec{r}_{12}^0 \mathbf{t}_{12} + t_{12}^0 \vec{r}_{12}}{U}$
$\mathbb{T}_{12} = \frac{2\mathbf{t}_{12} \otimes \mathbf{t}_{12} - \text{Tr}\{\mathbf{t}_{12} \otimes \mathbf{t}_{12}\} \mathbb{1}}{U}$	$\vec{\mathbb{T}}_{12} = -\frac{e}{V} \frac{\vec{r}_{12} \otimes \mathbf{t}_{12} + \mathbf{t}_{12} \otimes \vec{r}_{12} - \text{Tr}\{\vec{r}_{12} \otimes \mathbf{t}_{12}\} \mathbb{1}}{U}$

These are very general properties, which hold irrespectively on whether there is the inversion center connecting two atomic sites or not.

The inversion symmetry imposes an additional constraint on \hat{t}_{12} and \hat{r}_{12} . Namely, since \hat{t}_{12} is the (true) scalar and \hat{r}_{12} is the vector, the former should remain invariant under the permutation of atomic sites, while the latter changes its sign. Therefore, we should have:

$$\begin{aligned} t_{21}^0 &= t_{12}^0 & \mathbf{t}_{21} &= \mathbf{t}_{12} \\ \vec{r}_{21}^0 &= -\vec{r}_{12}^0 & \vec{r}_{21} &= -\vec{r}_{12}. \end{aligned} \quad (11)$$

Combining these properties with the hermiticity of \hat{t}_{12} and \hat{r}_{12} ,

$$\begin{aligned} t_{21}^0 &= t_{12}^0 & \mathbf{t}_{21} &= -\mathbf{t}_{12} \\ \vec{r}_{21}^0 &= \vec{r}_{12}^0 & \vec{r}_{21} &= -\vec{r}_{12}, \end{aligned} \quad (12)$$

we find that, in the centrosymmetric case, $\mathbf{t}_{12} = 0$ and $\vec{r}_{12}^0 = 0$. Thus, amongst all possible contributions to exchange interactions and electric polarization (Table 1), the finite ones will be only the isotropic exchange,

$$J_{12} = -\frac{(t_{12}^0)^2}{U} \quad (13)$$

and the antisymmetric (centrosymmetric) contribution to the polarization driven by the parameter:

$$\vec{\mathcal{P}}_{12}^C = -\frac{2e}{V} \frac{t_{12}^0 \vec{r}_{12}}{U}. \quad (14)$$

Another (noncentrosymmetric) contribution to the antisymmetric coupling,

$$\vec{\mathcal{P}}_{12}^N = -\frac{2e}{V} \frac{\vec{r}_{12}^0 \mathbf{t}_{12}}{U}, \quad (15)$$

will vanish, so as other contributions to the polarization of isotropic and symmetric anisotropic types. $\vec{\mathcal{P}}_{12}^N$ is entirely related to the crystallographic breaking of inversion symmetry in the bond and proportional to the DM interaction, $\vec{\mathcal{P}}_{12}^N \propto \vec{r}_{12}^0 D_{12}$.

Thus, the noncollinear alignment of spins in the centrosymmetric bond will induce the polarization $\vec{P} = \vec{\mathcal{P}}_{12}^C \cdot [\mathbf{e}_1 \times \mathbf{e}_2]$. If the exchange coupling J_{12} is antiferromagnetic (<0), the noncollinearity itself can be induced by the magnetic field \mathbf{H} , which is the essence of the conventional magnetoelectric effect resulting in $\vec{P} \sim \mathbf{H}$ [5]. In periodic solids, the noncollinearity may arise from the competition of isotropic exchange interactions J_{ij} in several bonds. Such situation is realized in multiferroic materials of the spin-spiral

type [16]. Nevertheless, in both cases, the microscopic origin of the electric polarization is the same and the polarization itself is proportional to $t_{ij}^0 \vec{r}_{ij}$.

Alternatively, the external electric field, \vec{E} , interacting with $\vec{\mathcal{P}}_{12}^C$, will produce the DM interaction $D_{12} = -\vec{E} \cdot \vec{\mathcal{P}}_{12}^C$, resulting in a noncollinear alignment of spins. Thus, the DM interactions and the magnetically induced polarization are closely related to each other. The microscopic mechanism of electric polarization induced by the noncollinear alignment of spins is sometimes called the inverse DM mechanism.

The first microscopic theory of electric polarization induced by the noncollinear alignment of spins was proposed by KNB [16], which also deals with the behavior of position operator \vec{r} in the basis of Kramers states. However, the KNB theory was also supplemented with several additional assumptions, which are, in principle, not needed:

- The oxygen states, which were explicitly considered by KNB [16], do not play an essential role for understanding the microscopic mechanism of emergence the electric polarization and can be eliminated from the model;
- KNB have considered a very special type of the Kramers doublet: $j = \frac{1}{2}$ states of the Γ_7 symmetry, which are split off by the spin-orbit interaction in the t_{2g} manifold. Formally, such assumption is not necessary as the behavior of electric polarization is related to more fundamental properties of \hat{t}_{12} and \hat{r}_{12} under the spatial inversion. Furthermore, the behavior of electric polarization depends on the symmetry of the Kramers states and appears to be less universal, as it may follow from the KNB paper [16]. We will return to this point in Section 8.

5. Lack of Crystallographic Inversion Symmetry as Manifestation of Antiferro Orbital Ordering

In this section we will briefly discuss the connection of additional term $\vec{\mathcal{P}}_{12}^N$, which appears in the noncentrosymmetric case, with the orbital ordering effects [28]. The latter are typically considered in the context of Jahn-Teller distortion. They also control the sign of interatomic exchange interactions, known as Goodenough–Kanamori–Anderson (GKA) rules [29–32]. The spatial inversion about the midpoint of the bond guarantees that the Kramers doublets at two edges of the bond are the same and transformed to each other by \mathcal{I} . Since each doublet can be visualized via the distribution of associated with it electron density, one can say that in this case we deal with the ferro orbital order: in an analogy with the FM spin order, where two spins are the same, here we deal the same electron densities. The electric polarization in this case is controlled solely by $\vec{\mathcal{P}}_{12}^C$. The lack of crystallographic inversion symmetry means that the Kramers doublets are different. Therefore, one can say that we deal with some kind of antiferro orbital order, again in terms of distribution of the electron densities. The new aspect in the context of GKA rules is that the antiferro orbital always order breaks the inversion symmetry of the bond [33]. Therefore, the antiferro orbital order, which is always noncentrosymmetric, is responsible not only for the FM coupling between the spins, as it is suggested by canonical GKA rules, but also induces the DM interaction and electric polarization in the bond. In the simplest microscopic model, where there is only one Kramers doublet, such polarization is proportional to \vec{r}_{12}^0 and the term $\vec{\mathcal{P}}_{12}^N$ in the expression for the antisymmetric coupling can be viewed as the manifestation of some antiferro orbital order.

6. Spin-1/2 and Single-Ion Anisotropies

The fundamental Kramers theorem states that, for the spin- $\frac{1}{2}$, there should be no single-ion contribution to the magnetic energy [34]. The same property holds for the magnetic dependence of electric polarization. The proof is extremely simple: for $i = j$

the hermiticity (12) yields: $t_{ii} = 0$ and $\vec{r}_{ii} = 0$, meaning that \hat{t}_{ii} as well as \hat{r}_{ii} are simply proportional to the 2×2 unity matrix $\hat{1}$. Then, neither Γ_{ii} nor $\tilde{\Gamma}_{ii}$ depends on the direction of spin.

For multiferroic materials, the single-ion contribution to the electric polarization is typically attributed to the spin-dependent metal-ligand hybridization [18,35]. The corresponding term is proportional to $(\hat{S} \cdot \vec{v})^2 \vec{v}$, where \vec{v} is the position of ligand atom relative to the transition-metal one with the spin \hat{S} . This contribution vanishes if the transition-metal atom is located in the inversion center (for each \vec{v} , there is a contribution with $-\vec{v}$). For the spin- $\frac{1}{2}$, $\hat{S} = \frac{1}{2}\hat{\sigma}$ and the properties of the Pauli matrices lead to the identity: $(\hat{S} \cdot \vec{v})^2 \vec{v} \sim \hat{1}$.

7. General Form of Position Operator in the Basis of Kramers States

Without the loss of generality, two states of the Kramers doublet can be taken in the form:

$$|+\rangle = |\psi^0 \uparrow\rangle + |\Delta\psi \downarrow\rangle \tag{16}$$

$$|-\rangle = |\psi^0 \downarrow\rangle - |\Delta\psi^* \uparrow\rangle, \tag{17}$$

where the symbols \uparrow and \downarrow explicitly stand for the spin part of these states, while ψ^0 and $\Delta\psi$ are the coordinate parts. Furthermore, ψ^0 can be viewed as the main component without SO coupling, while $\Delta\psi$ is induced by the SO coupling. By appropriately choosing the phases, ψ^0 can be taken as real, while $\Delta\psi$ can be complex. Thus, Equations (16) and (17) can be formally rewritten as:

$$|+\rangle = |\psi^0 \uparrow\rangle + |\text{Re}\Delta\psi \downarrow\rangle + i|\text{Im}\Delta\psi \downarrow\rangle \tag{18}$$

$$|-\rangle = |\psi^0 \downarrow\rangle - |\text{Re}\Delta\psi \uparrow\rangle + i|\text{Im}\Delta\psi \uparrow\rangle. \tag{19}$$

If $\mathcal{T} = i\hat{\sigma}^y \hat{K}$ is the time-reversal operator (where K stands for the complex conjugation), it holds $\mathcal{T}|+\rangle = -|-\rangle$ and $\mathcal{T}|-\rangle = |+\rangle$. The typical examples are the $j = 1/2$ (Γ_7) states [16],

$$|+\rangle = \frac{1}{\sqrt{3}}(|xy \uparrow\rangle + |yz \downarrow\rangle + i|zx \downarrow\rangle) \tag{20}$$

$$|-\rangle = \frac{1}{\sqrt{3}}(|xy \downarrow\rangle - |yz \uparrow\rangle + i|zx \uparrow\rangle), \tag{21}$$

or the z^2 states [26]

$$|+\rangle = \frac{1}{\sqrt{1+2\zeta^2}}(|z^2 \uparrow\rangle + i\zeta|yz \downarrow\rangle + \zeta|zx \downarrow\rangle) \tag{22}$$

$$|-\rangle = \frac{1}{\sqrt{1+2\zeta^2}}(|z^2 \downarrow\rangle + i\zeta|yz \uparrow\rangle - \zeta|zx \uparrow\rangle) \tag{23}$$

(ζ being the ratio of SO coupling to the crystal field splitting).

In order to find the expressions for \vec{r}_{ij}^0 and $\vec{r}_{ij} = (\vec{r}_{ij}^x, \vec{r}_{ij}^y, \vec{r}_{ij}^z)$, one have to consider matrix elements of \vec{r} in the basis of the Kramers states $|+\rangle$ and $|-\rangle$ at the sites i and j (see Supplementary Material):

$$\begin{aligned} \langle i + |\vec{r}|j+ \rangle &= \langle \psi_i^0 | \vec{r} | \psi_j^0 \rangle + \langle \text{Re}\Delta\psi_i | \vec{r} | \text{Re}\Delta\psi_j \rangle + \langle \text{Im}\Delta\psi_i | \vec{r} | \text{Im}\Delta\psi_j \rangle \\ &\quad + i \langle \text{Re}\Delta\psi_i | \vec{r} | \text{Im}\Delta\psi_j \rangle - i \langle \text{Im}\Delta\psi_i | \vec{r} | \text{Re}\Delta\psi_j \rangle, \end{aligned} \quad (24)$$

$$\begin{aligned} \langle i + |\vec{r}|j- \rangle &= -\langle \psi_i^0 | \vec{r} | \text{Re}\Delta\psi_j \rangle + \langle \text{Re}\Delta\psi_i | \vec{r} | \psi_j^0 \rangle \\ &\quad + i \langle \psi_i^0 | \vec{r} | \text{Im}\Delta\psi_j \rangle - i \langle \text{Im}\Delta\psi_i | \vec{r} | \psi_j^0 \rangle, \end{aligned} \quad (25)$$

$$\begin{aligned} \langle i - |\vec{r}|j+ \rangle &= \langle \psi_i^0 | \vec{r} | \text{Re}\Delta\psi_j \rangle - \langle \text{Re}\Delta\psi_i | \vec{r} | \psi_j^0 \rangle + \\ &\quad i \langle \psi_i^0 | \vec{r} | \text{Im}\Delta\psi_j \rangle - i \langle \text{Im}\Delta\psi_i | \vec{r} | \psi_j^0 \rangle, \end{aligned} \quad (26)$$

$$\begin{aligned} \langle i - |\vec{r}|j- \rangle &= \langle \psi_i^0 | \vec{r} | \psi_j^0 \rangle + \langle \text{Re}\Delta\psi_i | \vec{r} | \text{Re}\Delta\psi_j \rangle + \langle \text{Im}\Delta\psi_i | \vec{r} | \text{Im}\Delta\psi_j \rangle \\ &\quad - i \langle \text{Re}\Delta\psi_i | \vec{r} | \text{Im}\Delta\psi_j \rangle + i \langle \text{Im}\Delta\psi_i | \vec{r} | \text{Re}\Delta\psi_j \rangle. \end{aligned} \quad (27)$$

Then, decomposing

$$\hat{r}_{ij} = \begin{pmatrix} \langle i + |\vec{r}|j+ \rangle & \langle i + |\vec{r}|j- \rangle \\ \langle i - |\vec{r}|j+ \rangle & \langle i - |\vec{r}|j- \rangle \end{pmatrix}$$

in terms of the unity $\hat{1}$ and the vector of Pauli matrices $\hat{\sigma}$, it is straightforward to find that

$$\vec{r}_{ij}^0 = \langle \psi_i^0 | \vec{r} | \psi_j^0 \rangle + \langle \text{Re}\Delta\psi_i | \vec{r} | \text{Re}\Delta\psi_j \rangle + \langle \text{Im}\Delta\psi_i | \vec{r} | \text{Im}\Delta\psi_j \rangle, \quad (28)$$

$$\vec{r}_{ij}^x = \langle \psi_i^0 | \vec{r} | \text{Im}\Delta\psi_j \rangle - \langle \text{Im}\Delta\psi_i | \vec{r} | \psi_j^0 \rangle, \quad (29)$$

$$\vec{r}_{ij}^y = -\langle \psi_i^0 | \vec{r} | \text{Re}\Delta\psi_j \rangle + \langle \text{Re}\Delta\psi_i | \vec{r} | \psi_j^0 \rangle, \quad (30)$$

$$\vec{r}_{ij}^z = \langle \text{Re}\Delta\psi_i | \vec{r} | \text{Im}\Delta\psi_j \rangle - \langle \text{Im}\Delta\psi_i | \vec{r} | \text{Re}\Delta\psi_j \rangle. \quad (31)$$

As expected (see Section 4), \vec{r}_{ij}^0 is symmetric with respect to the permutation of i and j : $\vec{r}_{ji}^0 = \vec{r}_{ij}^0$, while \vec{r}_{ij} is antisymmetric: $\vec{r}_{ji} = -\vec{r}_{ij}$.

If $\text{Re}\Delta\psi_j$ and $\text{Im}\Delta\psi_j$ are induced by the SO interaction, \vec{r}_{ij}^x and \vec{r}_{ij}^y are of the first order in the SO coupling, while \vec{r}_{ij}^z is of the second order.

8. Symmetry Properties of Position Operator in the Basis of Kramers States

Since the electric polarization in the centrosymmetric bonds is proportional to \vec{r}_{ij} , in this sections we closely examine the symmetry properties of this tensor. The bond ij is assumed to be along the z axis, unless it is specified otherwise.

8.1. Crystallographic Symmetry Properties

First, let us consider the properties of \vec{r}_{ij} under the symmetry operations of the groups C_4 and C_2 . C_4 contains four symmetry elements: the 90° -, 180° -, and 270° -rotations about z (respectively, \hat{R}^1 , \hat{R}^2 , and \hat{R}^3), and the unity $\hat{R}^0 = \hat{E}$. C_2 is just the subgroup of C_4 , containing only \hat{E} and \hat{R}^2 . Our main goal here is to elucidate the differences in the behavior of \vec{r}_{ij} when the symmetry is lowered from C_4 to C_2 . Understanding these differences is crucial for understanding limitations of the KNB expression $\vec{P} \sim \vec{\epsilon}_{ji} \times [\mathbf{e}_i \times \mathbf{e}_j]$ for the magnetically induced polarization [16].

Each symmetry operation \hat{R}^n combines rotations in the spin (S) and orbital (L) subspaces: $\hat{R}^n = \hat{R}_L^n \hat{R}_S^n$, where \hat{R}_S^n are the 2×2 matrices of $SU(2)$ rotations [36], which are listed in Table 2.

Table 2. Transformations under the 90°, 180°, and 270°-rotations about z. Each symmetry operation combines rotations in spin (S) and orbital (L) subspaces: $\hat{R}^n = \hat{R}_S^n \hat{R}_L^n$. The spin matrices \hat{R}_S^n are listed in the right column of the Table. They specify how \hat{R}_L^n act on the coordinate part (Re $\Delta\psi$, Im $\Delta\psi$) of Kramers states. The same \hat{R}_L^n describes the transformation of x, y, and z. The upper sign in (Re $\Delta\psi$, Im $\Delta\psi$) corresponds to the even representation of the group C₄, while the lower sign corresponds to the odd one.

Rotation	$\hat{R}_L^n(x, y, z)$	$\hat{R}_L^n(\text{Re}\Delta\psi, \text{Im}\Delta\psi)$	\hat{R}_S^n
90°	(−y, x, z)	(∓Im $\Delta\psi$, ±Re $\Delta\psi$)	$\begin{pmatrix} e^{i\frac{\pi}{4}} & 0 \\ 0 & e^{-i\frac{\pi}{4}} \end{pmatrix}$
180°	(−x, −y, z)	(−Re $\Delta\psi$, −Im $\Delta\psi$)	$\begin{pmatrix} e^{i\frac{\pi}{2}} & 0 \\ 0 & e^{-i\frac{\pi}{2}} \end{pmatrix}$
270°	(y, −x, z)	(±Im $\Delta\psi$, ∓Re $\Delta\psi$)	$\begin{pmatrix} e^{i\frac{3\pi}{4}} & 0 \\ 0 & e^{-i\frac{3\pi}{4}} \end{pmatrix}$

Then, using this explicit form of \hat{R}_S^n , one can find how the coordinate part of the Kramers states will be transformed by \hat{R}_L^n . Indeed, acting by \hat{R}^1 on $|\pm\rangle$, one finds:

$$\begin{aligned} \hat{R}^1|+\rangle &= e^{i\frac{\pi}{4}} \hat{R}_L^1(|\psi^0 \uparrow\rangle - i|\Delta\psi \downarrow\rangle) \\ \hat{R}^1|-\rangle &= e^{-i\frac{\pi}{4}} \hat{R}_L^1(|\psi^0 \downarrow\rangle - i|\Delta\psi^* \uparrow\rangle). \end{aligned} \tag{32}$$

Moreover, without SO coupling, \hat{R}_L^1 should transform $|\psi^0\rangle$ to itself, apart from the phase: $\hat{R}_L^1|\psi^0\rangle = \pm|\psi^0\rangle$, where the sign depends on whether $|\psi^0\rangle$ forms even or odd representation of the group C₄ (for instance, it is “−” for the $j = 1/2$ states and “+” for the z^2 ones). Then, the requirement that $\hat{R}^1|+\rangle$ should coincide with $|+\rangle$ apart from the phase, leads to the following symmetry properties for the coordinate part:

$$\begin{aligned} \hat{R}_L^1|\text{Re}\Delta\psi\rangle &= \mp|\text{Im}\Delta\psi\rangle \\ \hat{R}_L^1|\text{Im}\Delta\psi\rangle &= \pm|\text{Re}\Delta\psi\rangle. \end{aligned} \tag{33}$$

The transformation properties under \hat{R}^2 and \hat{R}^3 can be obtained in the same way (see Supplementary Material). The results are summarized in Table 2 together with the transformation of x, y, and z by \hat{R}_L^n .

Then, we are ready to find which matrix elements of \vec{r}_{ij} remain invariant under the symmetry operations of the group C₂. Technically, this can be done by symmetrizing \vec{r}_{ij} :

$$\vec{r}_{ij} \rightarrow \frac{1}{2} \sum_{n=0,2} \hat{R}_L^n \vec{r}_{ij}$$

where \hat{R}_L^n acts both on the coordinate part of the Kramers states and \vec{r} . Then, x and y change the sign under \hat{R}_L^2 (see Table 2), while z does not. Furthermore, the combination of ψ^0 and either Re or Im parts of $\Delta\psi$ changes the sign, while any combination of the Re or Im parts of $\Delta\psi$ does not change the sign. Therefore, the tensor \vec{r}_{ij} should have the following form:

$$\vec{r}_{ij} = \begin{pmatrix} r_{ij}^{x,x} & r_{ij}^{x,y} & 0 \\ r_{ij}^{y,x} & r_{ij}^{y,y} & 0 \\ 0 & 0 & r_{ij}^{z,z} \end{pmatrix}, \tag{34}$$

in agreement with the previous finding [37,38]. Thus, $r_{ij}^{z,z}$ can be finite and induce the polarization even if the spins are perpendicular to the bond, so that $[e_i \times e_j]$ is parallel to z , as in the proper screw spiral. The polarization in this case is also expected to be parallel to z . Nevertheless, the effect is expected to be small, being only of the second order in the SO coupling (see Section 7). The C_2 symmetry does not impose any other constraints on the matrix elements of the xy block of \vec{r}_{ij} .

For the C_4 group, the symmetrization takes the form:

$$\vec{r}_{ij} \rightarrow \frac{1}{4} \sum_{n=0}^3 \hat{R}_L^n \vec{r}_{ij},$$

where we have to consider two additional symmetry elements \hat{R}_L^1 and \hat{R}_L^3 . Then, it is straightforward to find that (see Supplementary Material):

$$\vec{r}_{ij} = \begin{pmatrix} r_{ij}^{x,x} & -r_{ij}^{y,x} & 0 \\ r_{ij}^{y,x} & r_{ij}^{x,x} & 0 \\ 0 & 0 & r_{ij}^{z,z} \end{pmatrix}, \quad (35)$$

where

$$r_{ij}^{x,x} = \frac{1}{2} \left(\langle \psi_i^0 | x | \text{Im} \Delta \psi_j \rangle - \langle \text{Im} \Delta \psi_i | x | \psi_j^0 \rangle - \langle \psi_i^0 | y | \text{Re} \Delta \psi_j \rangle + \langle \text{Re} \Delta \psi_i | y | \psi_j^0 \rangle \right), \quad (36)$$

$$r_{ij}^{y,x} = \frac{1}{2} \left(\langle \psi_i^0 | y | \text{Im} \Delta \psi_j \rangle - \langle \text{Im} \Delta \psi_i | y | \psi_j^0 \rangle + \langle \psi_i^0 | x | \text{Re} \Delta \psi_j \rangle - \langle \text{Re} \Delta \psi_i | x | \psi_j^0 \rangle \right), \quad (37)$$

and

$$r_{ij}^{z,z} = \langle \text{Re} \Delta \psi_i | z | \text{Im} \Delta \psi_j \rangle - \langle \text{Im} \Delta \psi_i | z | \text{Re} \Delta \psi_j \rangle. \quad (38)$$

Thus, in comparison with the C_2 group, we have two additional symmetry constraints: $r_{ij}^{x,x} = r_{ij}^{y,y}$ and $r_{ij}^{y,x} = -r_{ij}^{x,y}$. Similar analysis performed for the group C_3 , which includes the 120° and 240° rotations about z , and \hat{E} , yields the same expression for \vec{r}_{ij} (see Supplementary Material).

Finally, applying symmetry operations of the groups C_4 and C_3 to $\text{Re} \Delta \psi$ and $\text{Im} \Delta \psi$ on the same site, it is straightforward to find that the Re and Im parts of $\Delta \psi$ are orthogonal to each other:

$$\langle \text{Re} \Delta \psi | \text{Im} \Delta \psi \rangle = \langle \text{Im} \Delta \psi | \text{Re} \Delta \psi \rangle = 0. \quad (39)$$

Nevertheless, this is not necessarily the case for the C_2 symmetry.

These are the properties of \vec{r}_{ij} , which are expected from the viewpoint of crystallographic symmetry. Particularly, even for the high symmetries, C_3 and C_4 , a finite $r_{ij}^{z,z}$ is expected from the crystallographic point of view. This was noticed by Dzyaloshinskii in his pioneering work [5]: besides the perpendicular magnetoelectric effect in Cr_2O_3 , he also predicted the longitudinal one, in the direction of the threefold rotation axis. Nevertheless, besides overt crystallographic symmetries there are also hidden ones, which enforce $r_{ij}^{z,z}$ (and some other matrix elements) to be zero for sufficiently high symmetries. These effects we will consider in the next section.

8.2. Hidden Symmetry Properties

This set of properties is related to the explicit dependence of $\text{Re} \Delta \psi$ and $\text{Im} \Delta \psi$ on the azimuthal angle φ in the bond. In the cylindrical coordinates, $x \sim \cos \varphi$ and $y \sim \sin \varphi$, and the 90° -, 180° -, and 270° -rotations about z , correspond to the transformations $\varphi \rightarrow \varphi + \frac{\pi}{2}$, $\varphi \rightarrow \varphi + \pi$, and $\varphi \rightarrow \varphi + \frac{3\pi}{2}$, respectively. Then, for the even representation

of C_4 , $\text{Re}\Delta\psi$ and $\text{Im}\Delta\psi$ transform as, respectively, x and y (see Table 2). Therefore, it is reasonable to assume that $\text{Re}\Delta\psi$ and $\text{Im}\Delta\psi$ should depend on φ as $\cos\varphi$ and $\sin\varphi$, respectively, while ψ^0 does not depend on φ . For the odd representation, $\text{Re}\Delta\psi$ and $\text{Im}\Delta\psi$ transform as, respectively, y and x . Therefore, it is reasonable to assume that $\text{Re}\Delta\psi \sim \sin\varphi$ and $\text{Im}\Delta\psi \sim \cos\varphi$. Moreover, ψ^0 for the odd case transform as $\sin 2\varphi$. Then, the integration over φ results in the following property: $r_{ij}^{x,x} = r_{ij}^{y,y} = r_{ij}^{z,z} = 0$, which is valid both for even and odd representations. Therefore, the only nonvanishing element of \vec{r}_{ij} is $r_{ij}^{y,x}$, which is given by:

$$r_{ij}^{y,x} = \langle \psi_i^0 | y | \text{Im}\Delta\psi_j \rangle - \langle \text{Im}\Delta\psi_i | y | \psi_j^0 \rangle = \langle \psi_i^0 | x | \text{Re}\Delta\psi_j \rangle - \langle \text{Re}\Delta\psi_i | x | \psi_j^0 \rangle.$$

Thus, for the C_4 symmetry, the tensor \vec{r}_{ij} becomes:

$$\vec{r}_{ij} = \begin{pmatrix} 0 & -r_{ij}^{y,x} & 0 \\ r_{ij}^{y,x} & 0 & 0 \\ 0 & 0 & 0 \end{pmatrix}, \tag{40}$$

which leads to the well-known expression $\vec{P} \sim \vec{e}_i \times [\mathbf{e}_i \times \mathbf{e}_j]$ [16,26]. The same expression can be obtained for the C_3 symmetry (see Supplementary Material). Particularly, since z does not depend on φ , the property $r_{ij}^{z,z} = 0$ results from the orthogonality condition between $\text{Re}\Delta\psi$ and $\text{Im}\Delta\psi$ for the high symmetries C_4 and C_3 [see Equation (39)].

For the group C_2 , there is only one symmetry operation, \hat{R}_L^2 , which changes the sign of x , y , $\text{Re}\Delta\psi$, and $\text{Im}\Delta\psi$ (see Table 2). In the other words, all four quantities obey the same transformation law. In such a situation, each of $\text{Re}\Delta\psi$ and $\text{Im}\Delta\psi$ can be the linear combination of $\cos\varphi$ and $\sin\varphi$. Then, the tensor \vec{r}_{ij} is generally given by Equation (34) with no additional hidden symmetry constraints, which would reduce the number of its independent matrix elements.

8.3. Order of Kramers States and Physical Properties

The asymmetric form of the tensor \vec{r}_{ij} is the key result of the KNB theory [16]. Nevertheless, this form depends on the order of the pseudospin states $|+\rangle$ and $|-\rangle$. To certain extend, it is a matter of choice which states are called “spin up” and which are “spin down”. Then, what will happen if one interchanges $|+\rangle$ with $|-\rangle$? Using the expressions for the matrix elements of \vec{r} in the basis of $|+\rangle$ and $|-\rangle$, Equations (24)–(27), and expanding \hat{r}_{ij} in terms of $\hat{1}$ and $\hat{\sigma}$, it is straightforward to see that the interchange of $|+\rangle$ and $|-\rangle$ will change the sign of \vec{r}_{ij}^y and \vec{r}_{ij}^z , but not the one of \vec{r}_{ij}^x . Therefore, the tensor \vec{r}_{ij} in this new representation becomes symmetric

$$\vec{r}_{ij} = \begin{pmatrix} 0 & \vec{r}_{ij}^{y,x} & 0 \\ \vec{r}_{ij}^{y,x} & 0 & 0 \\ 0 & 0 & 0 \end{pmatrix},$$

where $\vec{r}_{ij}^{y,x} = r_{ij}^{y,x}$, but $\vec{r}_{ij}^{x,y} = -r_{ij}^{x,y} = r_{ij}^{y,x} = \vec{r}_{ij}^{y,x}$. Such form of the tensor \vec{r}_{ij} was reported in Ref. [26] for the z^2 states. However, this is a consequence of specific order of the states $|+\rangle$ and $|-\rangle$. Therefore, there is no fundamental differences between the states $j = \frac{1}{2}$ (Γ_7) and z^2 : for the given C_4 symmetry, the tensor \vec{r}_{ij} should obey the same symmetry properties, irrespectively on the type of the basis states. Nevertheless, by changing the order of $|+\rangle$ and $|-\rangle$, one can switch between symmetric and antisymmetric representations.

Such a representation dependence of \vec{r}_{ij} is related to the properties of the pseudospin states. If $|\pm z\rangle \equiv |\pm\rangle$ are the pseudospine states in the positive and negative directions of z , corresponding to them pseudospin states in the positive and negative directions of x and

y are given by $|\pm x\rangle = \frac{1}{\sqrt{2}}|+\rangle \pm \frac{1}{\sqrt{2}}|-\rangle$ and $|\pm y\rangle = \pm \frac{1-i}{2}|+\rangle + \frac{1+i}{2}|-\rangle$, respectively [39]. Then, the interchange of $|+z\rangle$ and $|-z\rangle$ will also interchange the states $|+y\rangle$ and $|-y\rangle$ (apart from a phase) but not the states $|+x\rangle$ and $|-x\rangle$, thus explaining why \vec{r}_{ij}^y and \vec{r}_{ij}^z change the sign, while \vec{r}_{ij}^x does not change it.

Of course, the physical properties should not depend on the representation used for the pseudospin states. In reality, the magnetic system is probed by the magnetic field H . For instance, such field controls the direction of the spin canting in the conventional magnetoelectric effect [5] or the orientation of the spin rotation plane in spiral multiferroics [17]. The interaction $-\mu_B \mathcal{S}_i \cdot \mathcal{g}_i H$ of the pseudospin \mathcal{S}_i ($\mathcal{S}_i = \frac{1}{2}e_i$ for the single Kramers doublet) with H is mediated by the 3×3 g -tensor \mathcal{g}_i , which is given by the matrix elements of $\hat{\sigma}$ and angular momentum operator $\hat{L} = (\hat{L}^x, \hat{L}^y, \hat{L}^z)$ in the basis of pseudospin states [39]. Therefore, for the correct description of observable magnetoelectric properties, it is essential to use the same order of the pseudospin states in the definition of both tensors \vec{r}_{ij} and \mathcal{g}_i .

As an example, let us consider two canted spins, whose AFM component along z coexists with the FM one in the xy plane (Figure 2). The latter is induced by the magnetic field H , which can freely rotate in the xy plane. The corresponding directions of spins are given by $e_{1,2} = (\sin \theta \cos \varphi, \sin \theta \sin \varphi, \pm \cos \theta)$, in terms of the polar (θ) and azimuthal (φ) angles.

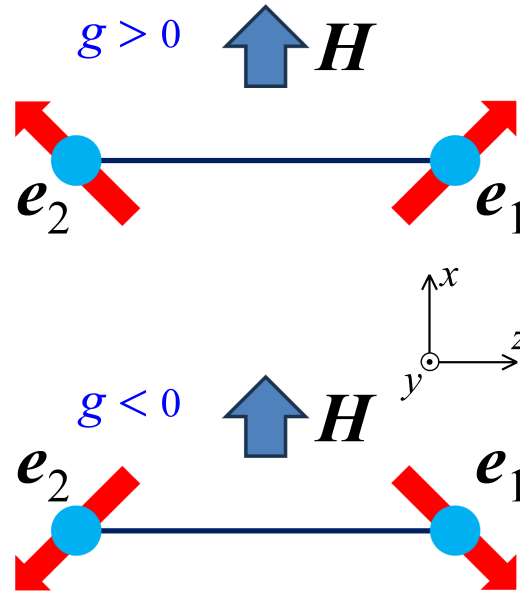


Figure 2. A cartoon picture explaining the canting of spins induced by the magnetic field depending on the sign of the g -factor.

For H along y ($\varphi = \frac{\pi}{2}$), the tensors \vec{r}_{12} and $\vec{\tilde{r}}_{12}$ produce the same polarization $\vec{P} = (0, P, 0)$ along y . Then, the rotation of $[e_1 \times e_2] = -\sin 2\theta(\sin \varphi, -\cos \varphi, 0)$ from x ($\varphi = \frac{\pi}{2}$) to $-y$ ($\varphi = 0$) would rotate $\vec{P} = (0, P, 0)$ to $\vec{P} = (P, 0, 0)$ in the case of \vec{r}_{12} and $\vec{P} = (-P, 0, 0)$ in the case of $\vec{\tilde{r}}_{12}$. The discrepancy is resolved by considering explicitly the g -tensor $\mathcal{g} = [g^{ab}]$ ($a, b = x, y, \text{ or } z$), which is diagonal and depends on the order of the pseudospin states such that $\tilde{g}^{yy} = g^{yy}$, but $\tilde{g}^{xx} = -g^{xx}$. Then, for $\mathcal{g} \cdot H || x$ will additionally change the sign of $[e_1 \times e_2]$ and, together with $\vec{\tilde{r}}_{12}$, produce $\vec{P} = (P, 0, 0)$, the same as for \vec{r}_{12} .

9. Other Contributions to \vec{P}

In the previous sections have considered the simplest microscopic theory of magnetoelectric coupling where the magnetically active states at each site of the lattice are represented by a single Kramers doublet. The key result of this theory is that, even in the crystallographically centrosymmetric bonds, the noncollinear alignment of spins can break

the inversion symmetry and induce the electric polarization. The tensor describing this magnetoelectric coupling, $\vec{\mathcal{P}}_{ij}^C$, is given by Equation (14) and its symmetry properties have been considered in Section 8. This finding further justifies and generalizes the KNB theory of the magnetoelectric coupling [16]. However, the situation realized in real materials can be more complex and it would not be entirely correct to analyse all the cases from the viewpoint of only this simplified model of the magnetoelectric coupling. In fact, there can be other mechanisms and all of them can be rigorously derived starting from the general expression (1) for the electric polarization in terms of the Wannier functions for the occupied bands [13–15].

First, if the bond is noncentrosymmetric, there will be an additional contribution to \vec{P} . The corresponding parameter $\vec{\mathcal{P}}_{ij}^N$, describing the antisymmetric magnetoelectric coupling, is given by Equation (15). It is obtained along the same line as $\vec{\mathcal{P}}_{ij}^C$, considering the intersite matrix elements of \vec{r}_{ij}^0 in the basis of Kramers states. $\vec{\mathcal{P}}_{ij}^N$ can also operate in the centrosymmetric systems, but where the inversion centers are not necessarily located in the midpoints of the bonds. The typical example is orthorhombic manganites, which will be considered in Section 10.2. Besides $\vec{\mathcal{P}}_{ij}^N$, the isotropic and symmetric anisotropic contributions to the polarization, which are driven by, respectively, \vec{P}_{ij} and $\vec{\mathbb{I}}_{ij}$, become finite in the noncentrosymmetric bonds.

Even more contributions are expected in the multiorbital case, where there is more than one Kramers doublet associated with each magnetic site. For instance, the noncentrosymmetric bond can be viewed as a dipole. Considering only two magnetic atoms at the edges of this bond (i and j in Figure 3) and disregarding explicit contributions of intermediate ligand sites, the electric dipole moment will be parallel to the bond. Mathematically, this approximation is obtained by replacing the r -space integration in Equation (1) by the summation over only two points i and j [23,24]. Then, one can control the charge transfer between i and j (and, therefore, the magnitude of the electric dipole moment in the bond) by realigning the spins at the sites i and j .

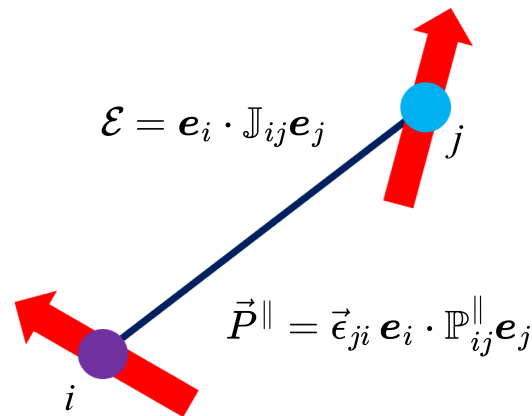


Figure 3. Modulation of electric polarization by the magnetic alignment in the noncentrosymmetric dipole. The direction of polarization is fixed along \vec{e}_{ji} (the unit vector along the dipole). However, the magnitude of the polarization can depend on the directions of spins \mathbf{e}_i and \mathbf{e}_j in the dipole, similar to the exchange energy.

The exchange energy in the noncentrosymmetric bond is given by $\mathbf{e}_i \cdot \mathbb{J}_{ij} \mathbf{e}_j$, where the 3×3 tensor \mathbb{J}_{ij} can be decomposed into isotropic (J_{ij}), DM (\mathbf{D}_{ij}), and symmetric anisotropic (\mathbb{I}_{ij}) parts. Then, the polarization will have a similar form, $\vec{e}_{ji} \mathbf{e}_i \cdot \mathbb{P}_{ij}^{\parallel} \mathbf{e}_j$, where \vec{e}_{ji} is the unit vector in the direction of the bond and the 3×3 tensor $\mathbb{P}_{ij}^{\parallel}$ can be further rearranged in terms of the isotropic, antisymmetric (DM-like), and symmetric anisotropic parts [23,40].

The microscopic mechanism behind $\mathbb{P}_{ij}^{\parallel}$ is essentially multi-orbital one. For each bond, $\mathbb{P}_{ij}^{\parallel}$ is proportional to $J_H \left((t_{ij}^{ab})^2 - (t_{ij}^{ba})^2 \right)$, where J_H is the intraatomic exchange (Hund's rule coupling) and t_{ij}^{ab} is the transfer integral between orbitals a and b [23,40]. Thus, the diagonal contributions with $a = b$ vanish, so that the considered mechanism does not operate in the one-orbital case. In the multi-orbital case, it is driven by the Hund's rule coupling J_H .

10. Examples and Classification

In this section we reconsider the classification of some magnetoelectric and multiferroic materials in terms of main microscopic mechanisms of magnetoelectric coupling:

- The generalized KNB mechanism (gKNB), where the inversion symmetry in the centrosymmetric bond can be broken by a noncollinear magnetic order [16]. Nevertheless, contrary to the conventional KNB mechanism, the direction of electric polarization is not necessary limited by the expression $\vec{P} \sim \vec{\epsilon}_{ji} \times [e_i \times e_j]$, which can be justified only for relatively high C_3 or C_4 symmetries of the bond;
- The single-ion mechanism, which is a generalization of spin-dependent metal–ligand hybridization mechanism [18,35];
- Other mechanisms, which can take place in noncentrosymmetric bonds.

It is true that the KNB mechanism is generic in the sense that it can operate in all types of compounds with a noncollinear magnetic structure. However, there can be many complications caused by other mechanisms and contributions.

10.1. Cr_2O_3

Cr_2O_3 is the canonical material exhibiting the magnetoelectric effect, which was theoretically proposed by Dzyaloshinskii in 1959 [5] and experimentally verified by Astrov in 1960 [41]. Cr_2O_3 crystallizes in corundum structure (the space group $R\bar{3}c$) with the inversion center connecting two pairs of Cr atoms in the unit cell (see Figure 4).

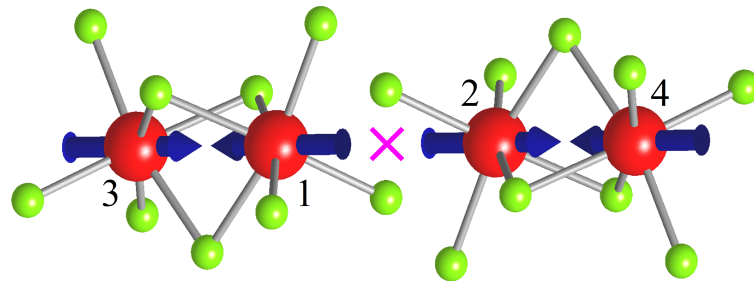


Figure 4. Fragment of crystal and magnetic structure of Cr_2O_3 . The directions of magnetic moments are denoted by arrows. The crystallographic inversion center is denoted by \times . Cr and O atoms are denoted by red and green spheres, respectively.

The magnetic moments are aligned antiferromagnetically, such that the pairs of sites 1 and 2 (3 and 4) are transformed to each other by the symmetry operation \mathcal{IT} . This symmetry can be broken by applying the magnetic field perpendicular to the bonds 12 and 34, resulting in net electric polarization. The bonds 12 and 34 have the C_3 symmetry. Therefore, the polarization in these bonds is expected to obey the conventional KNB rules, where the tensor \vec{r}_{ij} is given by Equation (40) and the polarization itself is proportional to $\vec{\epsilon}_{ji} \times [e_i \times e_j]$ [16]. In fact, this is rare case where the conventional KNB expression can be justified. In other multiferroic materials, which will be considered below, the bond symmetry is lower and we generally deal with a more complex form of the tensor \vec{P}_{ij} . In addition to the KNB mechanism, the single-ion contributions are also expected in the case of Cr_2O_3 , as we deal with the $S = \frac{3}{2}$ Cr^{3+} ions located in the noncentrosymmetric positions. Furthermore, the bonds 14 and 23 are noncentrosymmetric, that may activate

other mechanisms of the magnetoelectric coupling besides KNB and single-ion anisotropy. For instance, the antisymmetric exchange coupling in the bonds 14 and 23 is known to be responsible for the phenomenon of weak ferromagnetism in Fe_2O_3 , which has the same crystal structure but different type of AFM order [21]. Therefore, one could also expect a finite contribution of these bonds to the electric polarization \vec{P} [24]. Nevertheless, for the conventional magnetoelectric effect in Cr_2O_3 , the spins in the bonds 14 and 23 remain parallel. Therefore, there should be no contributions to \vec{P} arising from these noncentrosymmetric bonds, perhaps except small symmetric anisotropic ones. The results are summarized in Table 3.

Table 3. Summary of main microscopic mechanisms operating (or not) in real magnetoelectric (ME) or multiferroic (MF) materials: the KNB mechanism in centrosymmetric bonds, the single-ion (SI) mechanism, and other mechanisms emerging in noncentrosymmetric bonds. The KNB rules, relating the direction of electric polarization with the cross product of magnetic moments in the bond, are further specified in parentheses, where ‘c’ stands for the conventional KNB rules expected for high bond symmetries, and ‘g’ stands for the generalized rules expected for lower symmetries. If the SI mechanism does not operate, the reason is explained in parentheses: $S = 1/2$, or if the magnetic ions are located in inversion centers (denoted as ‘ic’), or both or them.

Material	Space Group	Type	KNB	SI	Other
Cr_2O_3	$R\bar{3}c$	ME	Yes (c)	Yes	No
TbMnO_3	$Pbnm$	MF	Yes (g)	No (ic)	Yes
MnWO_4	$P2/c$	MF	Yes (g)	Yes	Yes
CuCl_2	$C2/m$	MF	Yes (g)	No (ic and $S = 1/2$)	No
CuO	$C2/c$	MF	Yes (g)	No ($S = 1/2$)	Yes
$\text{Ba}_2\text{CoGe}_2\text{O}_7$	$P\bar{4}2_1m$	MF	No	Yes	No
$\text{Ba}_2\text{CuGe}_2\text{O}_7$	$P\bar{4}2_1m$	MF	Yes (g)	No ($S = 1/2$)	Yes
CuFeO_2	$R\bar{3}m$	MF	Yes (g)	No (ic)	No
MnI_2	$P\bar{3}m1$	MF	Yes (g)	No (ic)	No
$\text{RbFe}(\text{MoO}_4)_2$	$P\bar{3}$	MF	Yes (g)	No (ic)	No

10.2. TbMnO_3 and Other Multiferroic Manganites

TbMnO_3 is one of the first experimentally discovered multiferroic materials, where cycloidal magnetic order, developed in otherwise centrosymmetric orthorhombic crystal (the space group $Pbnm$), gives rise to spontaneous electric polarization [7]. The direction of this polarization depends on the orientation of the cycloidal plane and this dependence is well explained in terms of the conventional KNB theory. Particularly, the spin-spiral propagation vector in TbMnO_3 is $\vec{q} \approx (0, \frac{1}{4}, 0)$. Then, the spin spiral in the orthorhombic ab plane induces the polarization along the a axis, while the spin spiral in the plane bc induces the polarization along the c axis (see Figure 5). Thus, in both cases \vec{P} is proportional to $\vec{q} \times [\mathbf{e}_i \times \mathbf{e}_j]$, in agreement with the KNB theory [16].

In the ideal $Pbnm$ structure, the magnetic Mn^{3+} ions are located in the inversion centers, thus excluding single-ion contributions to the electric polarization. Nevertheless, in all other respects the situation is not such simple: The symmetry of the Mn-O-Mn bonds is low and all these bonds are noncentrosymmetric. Therefore, in addition to the conventional KNB mechanism, there can be other contributions to \vec{P} .

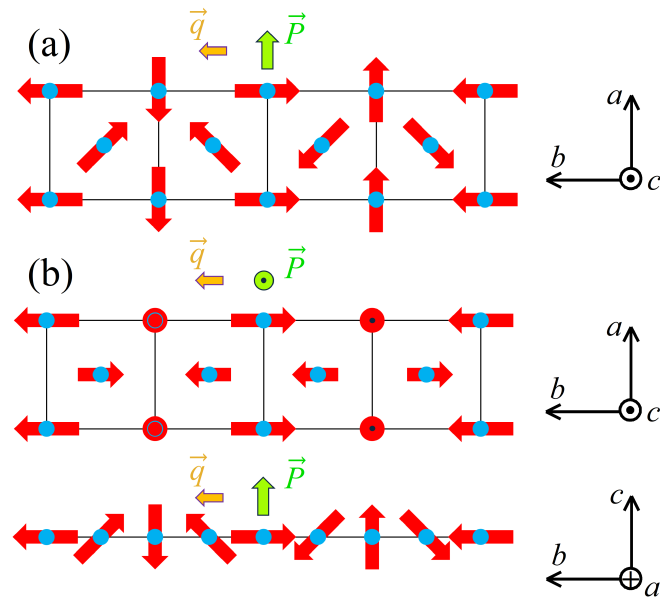


Figure 5. Magnetic cycloidal structures realized in TbMnO₃. (a) *ab* cycloid. (b) *bc* cycloid: the view in the *ab* plane (top) and in the *bc* plane (bottom). \vec{q} shows the propagation direction of the spin spiral. \vec{P} shows the corresponding direction of electric polarization.

Another complication arises from the fact that the spin-spiral texture in TbMnO₃ and related orthorhombic perovskite manganites can be deformed due to the large single-ion anisotropy, which tends to lock the spin spiral to the lattice and make it a commensurate one. If the regular spin-spiral texture is characterized by the same $e_i \cdot e_j$ in all the bonds, the deformation makes some of them inequivalent, including those, which were crystallographically connected by the spatial inversion (see Figure 6a) [42]. This gives rise to the additional, isotropic, contribution to \vec{P} in the case of the *ab* cycloid.

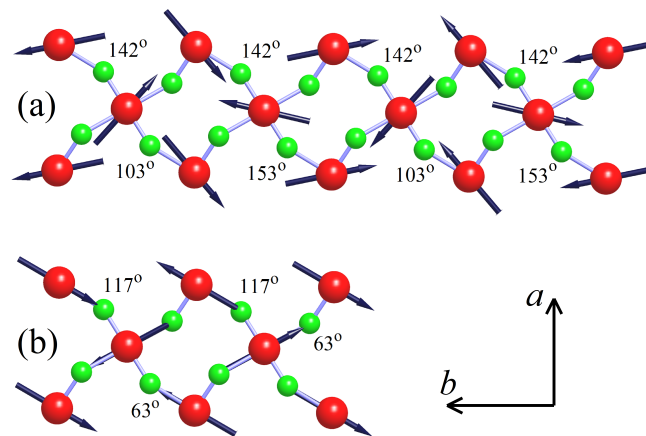


Figure 6. Magnetic textures obtained in the Hartree-Fock approximation for realistic electronic model (constructed for the Mn 3*d* bands in TbMnO₃) assuming (a) fourfold magnetic periodicity and (b) twofold magnetic periodicity [42]. Mn and O atoms are denoted by red and green spheres, respectively. Mn atoms are located in inversion centers.

This mechanism can be easily rationalized in terms of the double exchange model, which should be applicable for the high-spin ions, such as Mn³⁺ in manganites [43]. According to this model, the effect of noncollinear alignment of spins in the bond *ij* can be described by redefining the transfer integral as $\hat{t}_{ij} \rightarrow \zeta_{ij}\hat{t}_{ij}$, where $|\zeta_{ij}| = \sqrt{\frac{1+e_i \cdot e_j}{2}}$. Thus, if the bonds on opposite sides of the inversion center are characterized by different ζ_{ij} 's, the inversion symmetry will be broken. The mechanism appears to be generic and can be

applied to all types of magnetic textures, which can be viewed as a deformed spin spiral [44]. The example of such twofold periodic magnetic texture in orthorhombic manganites is shown in Figure 6b. It can be viewed as the spin spiral with $\vec{q} = (0, \frac{1}{2}, 0)$, which is deformed by the single-ion anisotropy term. The latter tends to align the spins along the longest Mn-O bond within the orthorhombic ab plane.

The special case of the twofold periodic magnetic texture in manganites is the collinear E-type AFM phase (see Figure 7), which is realized in HoMnO_3 [45] and YMnO_3 [46], and can be viewed as a limiting case of the deformed spin spiral with $\vec{q} = (0, \frac{1}{2}, 0)$.

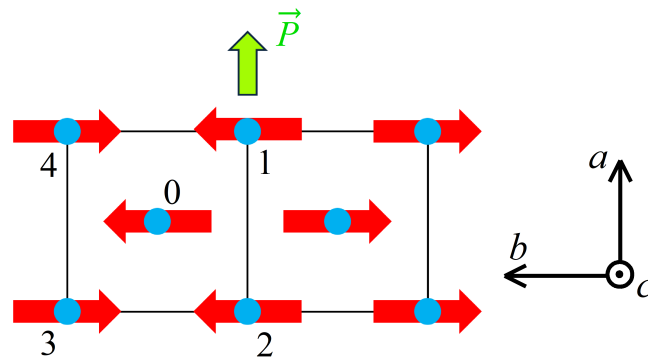


Figure 7. E-type antiferromagnetic texture realized in HoMnO_3 and YMnO_3 . \vec{P} shows the corresponding direction of electric polarization.

In this phase, two of the nearest bonds (01 and 02 in Figure 7) are ferromagnetic, while two other bonds (03 and 04, which are connected with 01 and 02 by the spatial inversion) are antiferromagnetic. Thus, according to the double exchange mechanism, the inversion symmetry is broken and the system develops a spontaneous polarization. Like in the noncollinear case (see Section 2), the inversion symmetry breaking in the E-phase occurs because some parts of the magnetic pattern are transformed to themselves by the symmetry operation \mathcal{IT} , while other parts require \mathcal{I} to be the symmetry operation, which is incompatible with \mathcal{IT} . Indeed, the sites 1 and 3 (2 and 4) can be transformed to each other by the symmetry operation \mathcal{IT} . However, such symmetry implies that the central site 0 should be nonmagnetic. Although such state is allowed from the symmetry point of view, for the high-spin ions Mn^{3+} , it would result in gigantic loss of the Hund’s rule energy. Thus, all Mn sites in the E-type AFM texture remain magnetic, but such type of the magnetism breaks the inversion symmetry.

The collinear alignment of spins in the E-phase is enforced by the exchange striction effects, associated with off-centrosymmetric displacements of Mn atoms [46,47]. The lattice displacements (the so-called inverse DM effect) are also expected in the spin-spiral phase of TbMnO_3 [48,49].

Thus, although the KNB mechanism is certainly relevant to the physics of TbMnO_3 and other multiferroic manganites, there are many other contributions affecting the behavior of electric polarization in this type of compounds.

10.3. MnWO_4 and Related Spin-Spiral Multiferroics with Low Crystallographic Symmetry

There are several spin-spiral multiferroics with relatively low crystallographic symmetry, including $\text{Ni}_3\text{V}_2\text{O}_8$ (space group $Cmca$) [50], FeVO_4 ($P\bar{1}$) [51], and MnWO_4 ($P2/c$) [52–54]. In this section we will briefly discuss some basic features of magnetoelectric coupling in MnWO_4 , which are inherent to the behavior of other spin-spiral multiferroics with low crystallographic symmetry.

MnWO_4 crystallizes in the monoclinic $P2/c$ structure, which is shown in Figure 8a, and develops the spiral magnetic order in the temperature range $7.6 \text{ K} \lesssim T \lesssim 12.5 \text{ K}$ with

the propagation vector $\vec{q} \approx (-\frac{1}{4}, \frac{1}{2}, \frac{1}{2})$, as explained in Figure 8b. Thus, the spin spiral propagates along the monoclinic a axis, while the magnetic coupling in two other directions is antiferromagnetic. The cross product $e_i \times e_j$ formed by neighboring spins lie in the ac plane. The spiral magnetic order induces the electric polarization along the b axis, that is formally consistent with the KNB rules [52]. The polarization vanishes in the collinear phases realized below 7.6 K and above 12.5 K.

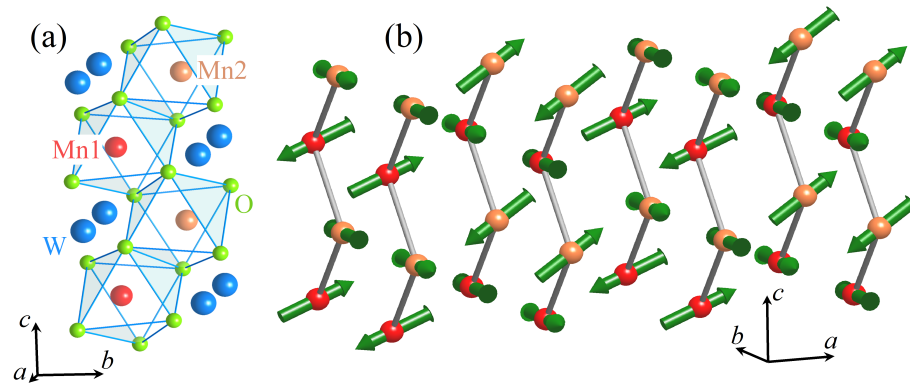


Figure 8. Fragment of crystal (a) and magnetic (b) structure of MnWO_4 in the noncollinear phase. Two Mn sublattices are shown by different colors.

Nevertheless, since the symmetry is low, there can be other contributions to the electric polarization. First, the KNB mechanism itself is expected to be of the generalized form, where other matrix elements of \vec{r}_{ij} can play some role. Then, the $P2/c$ structure of MnWO_4 has the inversion center, which connects two Mn sublattices with each other. In Figure 8, these sublattices are shown by different colors. Therefore, the bonds formed between the sublattices are centrosymmetric, while the bonds within each sublattice are not. In the latter case, there can be other contributions to \vec{P} : isotropic, \vec{P}_{12}^N , and symmetric anisotropic.

The spin-spiral alignment in MnWO_4 is caused by the competition of isotropic exchange interactions [55]. The DM interaction is forbidden between the sublattices, but can operate within each sublattice. For each bond \mathbf{R} connecting two Mn sites in the sublattice, the vectors of DM interactions in different sublattices are related by the identity $D^2(\mathbf{R}) = D^1(-\mathbf{R}) = -D^1(\mathbf{R})$, which describes the transformation of the axial vector under the spatial inversion. Then, from the viewpoint of DM interactions, the spins in different sublattices prefer to spiral in the opposite directions (say, clockwise and counterclockwise). However, the competing isotropic interactions, which are generally stronger than the DM ones, will establish the same type of spiral in both sublattices. Thus, in one sublattice, the isotropic and DM contributions to the spin spiral will be collaborative, while in another sublattice they will inevitably be competing. Thus, in the spin-spiral phase, the Mn sublattices become intrinsically nonequivalent, that by itself destroys the spatial inversion and contributes to the behavior of electric polarization [55].

10.4. CuCl_2 and CuBr_2

CuX_2 ($X = \text{Cl}$ or Br) are the only known so far multiferroic materials, where the KNB mechanism operates alone, without additional complications. They crystallize in the monoclinic $C2/m$ structure, consisting of the CuX_2 chains propagating along the b axis [56,57]. Competing isotropic exchange interactions stabilize the spin-spiral multiferroic phase with $\vec{q} \approx (1, \frac{1}{4}, \frac{1}{2})$ [26,56], as explained in Figure 9.

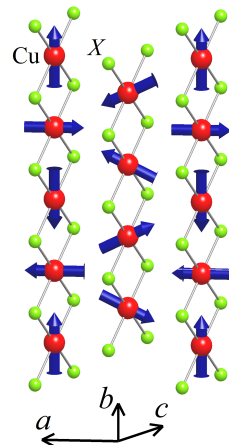


Figure 9. Fragment of crystal and magnetic structure of CuX_2 ($X = \text{Cl}$ or Br).

The magnetic Cu^{2+} ions are located in the inversion centers. Moreover, the nominal spin of Cu^{2+} is $S = 1/2$. Therefore, there is no single-ion contributions to the electric polarization. All Cu-Cu bonds are centrosymmetric. Nevertheless, the symmetry of the bonds is low; for the bonds in the chains, it is C_2 (where the rotation axis is b), while for other bonds there is no symmetry at all, apart from the inversion. Thus, we deal with the generalized KNB mechanism, where the 3×3 tensors \vec{r}_{ij} is specified by five elements for the bonds parallel to b and by all nine elements for other bonds. Nevertheless, the contributions in the chains clearly prevail [26]. Then, the polarization is expected to be in the ac plane, depending in the orientation of the spin-spiral plane, which can be controlled by the magnetic field [56].

10.5. CuO

Cupric oxide (CuO) is the promising multiferroic material. It crystallizes in the monoclinic $C2/c$ structure [58]. Similar to CuX_2 ($X = \text{Cl}$ or Br), the main structural pattern of CuO is the centrosymmetric CuO_2 chains propagating in the ab plane (Figure 10a). The basic difference is that in CuO there are two Cu sublattices (Cu1 and Cu2 in Figure 10), forming two distinct CuO_2 chains. Each sublattice can be transformed to itself by \mathcal{I} . However, different sublattices are not connected by \mathcal{I} .

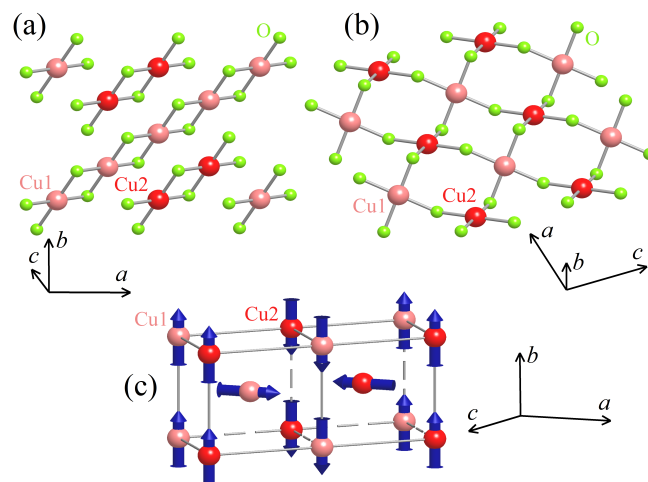


Figure 10. Crystal and magnetic structure of CuO . (a) The main structural pattern in the ab plane. (b) Fragment of the crystal structure in the ac plane. (c) Noncollinear magnetic structure with $\vec{q} \approx (\frac{1}{2}, 0, -\frac{1}{2})$ leading to the multiferroic behavior. Two Cu sublattices are shown by different colors.

At low temperatures, CuO is a collinear antiferromagnet. Nevertheless, when the temperature increases, it exhibits a transition to an incommensurate spin-spiral phase with $\vec{q} = (0.506, 0, -0.483)$ (Figure 10c) coexisting with the onset of multiferroic activity [58,59]. The Néel temperature is relatively high ($T_N = 230$ K) and can be further increased up to the room temperature by applying the hydrostatic pressure, as was suggested on the basis of first-principles electronic structure calculations [60] and directly verified in experiments on the neutron diffraction [59]. Thus, CuO can become a room-temperature multiferroic, where the electric polarization is induced by the noncollinear magnetic order.

The nominal spin of Cu^{2+} in CuO is again $S = 1/2$, suggesting that the single-ion anisotropy does not contribute to magnetic dependence of \vec{P} . Within centrosymmetric sublattices Cu1 and Cu2, the magnetic dependence of electric polarization can be described by the generalized KNB mechanism. However, since Cu1 and Cu2 are not connected by \mathcal{I} , the coupling between these sublattices should involve the additional contribution given by Equation (15).

10.6. $\text{Ba}_2\text{CoGe}_2\text{O}_7$ and $\text{Ba}_2\text{CuGe}_2\text{O}_7$

$\text{Ba}_2\text{CoGe}_2\text{O}_7$ and $\text{Ba}_2\text{CuGe}_2\text{O}_7$ crystallize in the noncentrosymmetric tetragonal $P\bar{4}2_1m$ structure (see Figure 11) [61,62].

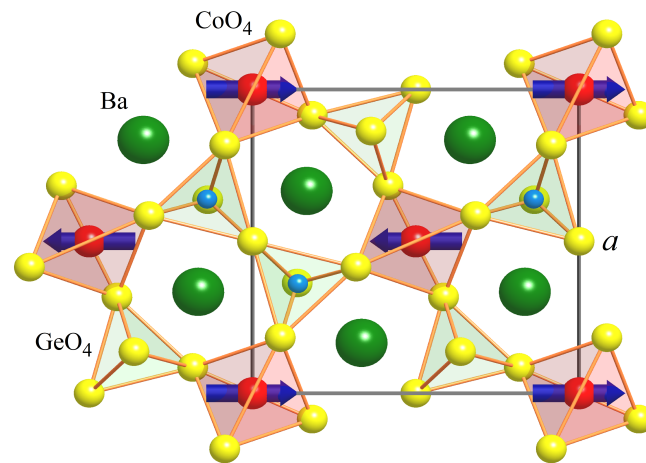


Figure 11. Crystal and magnetic structure of $\text{Ba}_2\text{CoGe}_2\text{O}_7$ in the tetragonal plane. a is the lattice parameter.

The crystal structure itself is non-polar due to the fourfold rotoinversion symmetry. Nevertheless, certain magnetic alignment can lower the symmetry and induce finite electric polarization. Besides the multiferroicity, the $P\bar{4}2_1m$ symmetry is responsible for a number of interesting effects, such as the coexistence of chiral magnetic ordering and weak ferromagnetism as well as the possibility of inducing the antiskyrmion textures [63].

From the viewpoint of magnetism, the main difference between $\text{Ba}_2\text{CoGe}_2\text{O}_7$ and $\text{Ba}_2\text{CuGe}_2\text{O}_7$ is the spin state of magnetic ions: $S = 3/2$ for Co^{2+} , while $S = 1/2$ for Cu^{2+} . Thus, the single-ion contributions to the exchange energy and electric polarization are expected in $\text{Ba}_2\text{CoGe}_2\text{O}_7$, but not in $\text{Ba}_2\text{CuGe}_2\text{O}_7$. This has a dramatic effect on the magnetic properties of these compounds. The single-ion anisotropy in $\text{Ba}_2\text{CoGe}_2\text{O}_7$ traps the magnetic moments in the xy plane and forces the nearly collinear AFM structure with $\vec{q}_0 = (1, 0, 0)$ (see Figure 11). The AFM coupling between nearest spins is driven by isotropic exchange interactions. Since the single-ion anisotropy energy for $S = 3/2$ in the tetragonal case does not depend on the azimuthal angle ϕ [64], this magnetic structure can be easily rotated in the xy plane by the magnetic field [35]. The DM interactions are permitted by the crystallographic symmetry. However, in $\text{Ba}_2\text{CoGe}_2\text{O}_7$ these interactions are overpowered by large single-ion anisotropy, resulting in collinear AFM alignment. In $\text{Ba}_2\text{CuGe}_2\text{O}_7$,

the single-ion anisotropy vanishes so that the DM interactions become active, leading to formation of the incommensurate spin-spiral phase with $\vec{q} = \vec{q}_0 + \delta\vec{q}$. The spin moments rotate in the plane specified by the vector $\vec{n}^\perp = (-\sin\phi, \cos\phi, 0)$, being perpendicular to the spin-rotation plane, and the spin-spiral deformation of the AFM $\vec{q}_0 = (1, 0, 0)$ structure is given by $\delta\vec{q} = \delta q(\sin\phi, \cos\phi, 0)$, where δq depends on the ratio of DM and isotropic exchange interactions between nearest neighbors in the xy plane [23]. In the other words, the spin spiral propagates in the xy plane, while the spins rotate in the plane formed by the z axis and one of the axes in the xy plane. The classical energy of the spin spiral does not depend on ϕ . Therefore, in order to find ϕ , it is essential to consider the effects of quantum zero-point motion, following the procedure of Yildirim et al. [65], which tend to stabilize the magnetization parallel to one of the square diagonals in the xy plane [23].

The KNB mechanism is not activated in $\text{Ba}_2\text{CoGe}_2\text{O}_7$, which is the collinear antiferromagnet. The magnetic dependence of \vec{P} in this case is almost solely given by the single-ion anisotropy: the rotation of magnetization in the xy plane destroys the rotoinversion symmetry, resulting in finite \vec{P} [25,35]. In the $S = \frac{1}{2}$ material $\text{Ba}_2\text{CuGe}_2\text{O}_7$, the single-ion anisotropy vanishes and the polarization is induced by the spin-spiral alignment via the generalized KNB mechanism. However, the spiral structure itself is driven by the DM interactions and emerges in the first order of the SO coupling. Therefore, the magnetic dependence of electric polarization is the second-order effect with respect to the SO coupling. Furthermore, all Cu-Cu bonds in $\text{Ba}_2\text{CuGe}_2\text{O}_7$ are noncentrosymmetric and besides KNB there can be other contributions to \vec{P} [23].

10.7. Triangular-Lattice Magnets

The triangular-lattice magnets CuFeO_2 [18], MnI_2 [19], and $\text{RbFe}(\text{MoO}_4)_2$ [20] have attracted a great deal of attention as examples of spin-spiral multiferroics, where the canonical KNB rules fail. Namely, the magnetic textures realized in CuFeO_2 and MnI_2 can be regarded as “proper screw”, where the moments rotate in the plane perpendicular to the spin-spiral propagation \vec{q} in the triangular plane (see Figure 12a,b).

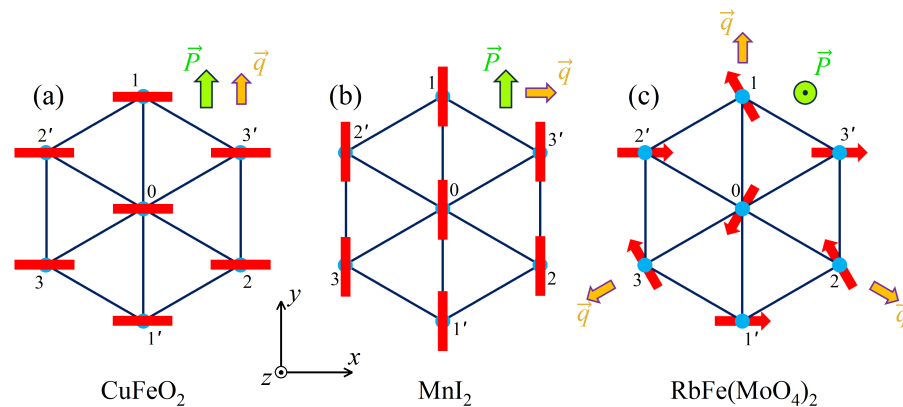


Figure 12. Different types of magnetic order on triangular lattices realized in CuFeO_2 (a), MnI_2 (b), and $\text{RbFe}(\text{MoO}_4)_2$ (c). \vec{q} shows the propagation direction of the spin spiral. In the 120° spin structure, realized in $\text{RbFe}(\text{MoO}_4)_2$, there are three equivalent directions of \vec{q} . \vec{P} shows corresponding direction of the electric polarization. In (a,b), the magnetic moments are rotated in the planes formed by the z axis and either x (a) or y (b) axis. These planes are indicated by thick red bars. In (c), the magnetic moments are in the xy plane and indicated by the red arrows.

Therefore, the construction $\vec{q} \times [\mathbf{e}_i \times \mathbf{e}_j]$ should vanish. There are two possible configurations, where: (i) the rotation plane is perpendicular to the bonds of the triangular lattice (see Figure 12a), which is realized in CuFeO_2 [18]; (ii) the rotation plane is parallel to the bonds of the triangular lattice (Figure 12b), which is realized in MnI_2 , in low

magnetic field [19]. Furthermore, in MnI_2 , the configuration shown in Figure 12a can be also realized in the high magnetic field, applied perpendicular to the rotation plane [19]. The proper screw magnetic order induces the electric polarization, that is rather unexpected from the viewpoint of KNB rules. The polarization remains parallel to the bonds for both types of magnetic structures shown in Figure 12a,b. In the 120° spin structure, realized in $\text{RbFe}(\text{MoO}_4)_2$, the magnetic moments rotate in the triangular plane. This magnetic structure can be described by three propagation vectors \vec{q} , which are parallel to the bonds (see Figure 12c). Therefore, according to KNB rules, for each bond, the polarization is expected to be in the plane and perpendicular to this bond, so that there will be a cancellation of contributions stemming from three bonds around each magnetic site. However, the experiment situation is again different: there is a finite polarization and it is perpendicular to the triangular plane [20].

These experimental data spurred the search of new mechanisms of the magnetoelectric coupling, which would explain the properties of triangular-lattice magnets. This mechanism was regarded to be the spin-dependent metal-ligand hybridization [17,18], which is some sort of the single-ion anisotropy as it does not depend on the relative alignment of spins on different magnetic sites. However, in all these materials, the magnetic atoms are located in the inversion centers. Therefore, the single-ion contributions to the electric polarization are forbidden by the symmetry.

Nevertheless, the behavior of CuFeO_2 , MnI_2 , and $\text{RbFe}(\text{MoO}_4)_2$ can be naturally understood by considering the generalized KNB mechanism for the magnetic bonds with relatively low symmetry [37,38]. Indeed, the bonds in the triangular plane are centrosymmetric. However, besides the spatial inversion, there is only twofold rotation in the case of CuFeO_2 and MnI_2 , and no other symmetries at all in the case of $\text{RbFe}(\text{MoO}_4)_2$.

In CuFeO_2 , the spin-spiral propagation vector can be taken parallel to y : $\vec{q} = (0, q^y, 0)$ (see Figure 12a). The spin-spiral plane is perpendicular to \vec{q} , both in CuFeO_2 and MnI_2 . Therefore, we have $[e_0 \times e_1] = (0, \sin q^y, 0)$ and $[e_0 \times e_2] = [e_0 \times e_3] = (0, -\sin \frac{q^y}{2}, 0)$, where \vec{q} is in the units of inverse lattice parameter. The symmetry properties of \vec{r}_{01} , \vec{r}_{02} , and \vec{r}_{03} in the nearest bonds, which are connected by the threefold rotation, are considered in supplementary materials (see Supplementary Material). Then, it is straightforward to find that $\vec{P} = (0, P^y, 0)$, where $P^y \sim r^{y,y} \sin q^y - \left(\frac{3}{2}r^{x,x} + \frac{1}{2}r^{y,y}\right) \sin \frac{q^y}{2}$. Furthermore, since $|r^{x,x}| \gg |r^{y,y}|$ ($r^{x,x}$ is of the first order in the SO coupling, while $r^{y,y}$ is only of the second order), one can write $P^y \sim -\frac{3}{2}r^{x,x} \sin \frac{q^y}{2}$.

In MnI_2 , \vec{q} is parallel to x : $\vec{q} = (q^x, 0, 0)$ (see Figure 12b). Then, $[e_0 \times e_1] = 0$ and this bond does not contribute to \vec{P} . For other two bonds we have $[e_0 \times e_2] = -[e_0 \times e_3] = \left(\sin \frac{\sqrt{3}q^x}{2}, 0, 0\right)$. Combining them with \vec{r}_{02} and \vec{r}_{03} (see Supplementary Material), it is again straightforward to find that $\vec{P} = (0, P^y, 0)$, where in the first order of the SO coupling $P^y \sim -\frac{\sqrt{3}}{2}r^{x,x} \sin \frac{\sqrt{3}q^x}{2}$.

For the 120° spin structure, realized in $\text{RbFe}(\text{MoO}_4)_2$ (see Figure 12c), we have $[e_0 \times e_1] = [e_0 \times e_2] = [e_0 \times e_3] = \left(0, 0, -\frac{\sqrt{3}}{2}\right)$, resulting in $\vec{P} = (0, 0, P^z)$, where $P^z \sim -\frac{\sqrt{3}}{2}r^{z,z}$.

Thus, the behavior of the triangular-lattice magnets CuFeO_2 , MnI_2 , and $\text{RbFe}(\text{MoO}_4)_2$ can be understood in terms of the generalized KNB mechanism. The two important points are: (i) the general form of the tensor \vec{r} , which in the case of the low symmetry can have finite diagonal elements; (ii) The geometry of magnetic bonds in the triangular lattice. Since all bonds are centrosymmetric, no additional complications are expected.

11. Summary and Outlook

We have considered basic principles of how the inversion symmetry can be broken by magnetic order, resulting in net electric polarization. The fundamental reason of such magnetic inversion symmetry breaking is the incompatibility of the FM and AFM order

patterns, which coexist in multiferroic systems. If the FM order parameter is invariant under the spatial inversion, $\mathcal{I}F = F$, the AFM ones requires the additional time reversal, $\mathcal{I}\mathcal{T}A = A$. Since \mathcal{I} cannot coexist with $\mathcal{I}\mathcal{T}$, the inversion symmetry is broken, that is manifested in appearance of the spontaneous polarization. The noncollinear alignment of spins is only one possible scenario where F coexists with A and there can be other possibilities besides the noncollinearity. For instance, the inversion symmetry breaking in the E phase of manganites is typically attributed to the exchange striction effects [6,8,17]. However, there is a more fundamental reason besides the exchange striction. This is again the incompatibility of the long-range AFM order in the Mn sublattice with the high-spin state of Mn^{3+} ions located in the inversion centers. For instance, this naturally explains the fact that, on the level of electronic structure calculations, the electric polarization can be readily obtained by imposing the E-type AFM order in the centrosymmetric orthorhombic structure without polar distortions [39,44,46,66]. Another example is GdFeO_3 , where G-type antiferromagnetically ordered Gd spins obey the magnetoelectric $\mathcal{I}\mathcal{T}$ symmetry, but the $\mathcal{I}\mathcal{T}$ symmetry operation is incompatible with magnetism of Fe atoms in the centrosymmetric positions [12].

This coexistence principle explains similarities and differences between the multiferroicity and magnetoelectricity, and how one can formally design multiferroic materials starting from magnetoelectric ones. The magnetoelectricity implies the AFM order, obeying the $\mathcal{I}\mathcal{T}$ symmetry: $\mathcal{I}\mathcal{T}A = A$. This symmetry operation can be broken by applying either electric or magnetic field, which induces simultaneously the ferroelectric polarization and ferromagnetic magnetization [5]. The multiferroicity is the phenomenon of the same type, but where the internal FM order parameter F plays the role of magnetic field, which breaks the $\mathcal{I}\mathcal{T}$ symmetry. Loosely speaking, the simplest recipe for making multiferroic material starting from the magnetoelectric one is to add a magnetic atom to the inversion center.

Although the internal FM order parameter F breaks time-reversal symmetry, it should not be confused with the phenomenon of weak ferromagnetism [21], which gave rise to a popular nowadays direction called “altermagnetism” [67]. The magnetoelectricity and weak ferromagnetism are two phenomena, emerging in unconventional AFM systems, where the magnetic unit cell coincides with the crystallographic one [5,21]. However, they are completely different from the viewpoint of symmetry and, generally, cannot coexist with each other: while the magnetoelectricity requires the spatial inversion \mathcal{I} to be always combined with \mathcal{T} , it must stand alone in the case of weak ferromagnetism [68,69]. The only possibility for such coexistence is when the magnetoelectricity and weak ferromagnetism emerge from different magnetic sublattices, as in GdFeO_3 and some other rare-earth perovskites, where the magnetoelectric Gd sublattice is combined with weakly ferromagnetic Fe sublattice [12,70].

The coexistence principle prescribes how the electric polarization \vec{P} should depend on the directions of spins. In the centrosymmetric bond, this dependence can be only in the form of the antisymmetric coupling between the spins and/or the single-ion anisotropy. No other contributions are formally allowed.

The microscopic picture behind these phenomenological principles can be derived by employing modern theory of the electric polarization [13–15]. For Mott multiferroics, whose electronic and magnetic properties are controlled by large on-site Coulomb repulsion, the modern theory can be further reformulated as the superexchange theory for the electric polarization. Nowadays, the modern theory of electric polarization is implemented in most of the electronic structure codes based on the density functional theory so that \vec{P} can be easily calculated without additional approximations supplementing the superexchange theory. Nevertheless, if we are interested in the *interpretation* of experimental data or results of electronic structure calculations, such approximations become very useful as they

provide a clear answer which microscopic invariant is responsible for finite \vec{P} in the case of noncollinear alignment of spins or any other scenario of magnetic inversion symmetry breaking. Namely, for the noncollinear alignment of spins, the magnetoelectric coupling in the centrosymmetric bond is controlled by the spin-dependent part of the position operator in the basis of Kramers states, \vec{r}_{12} .

The form of \vec{r}_{12} is not universal and depends on the symmetry of the bond. The symmetry properties of \vec{r}_{12} can be obtained by considering the symmetry of the Kramers states. Particularly, the commonly used KNB rule $\vec{P} \propto \vec{e}_{21} \times [e_1 \times e_2]$ can be justified only for relatively high rotational symmetry of the bond (threefold or higher). Considering the applicability of KNB rules to real multiferroic materials, the primary question is whether the magnetic bonds are centrosymmetric or not. If all bonds in the crystal are centrosymmetric, the KNB mechanism itself is applicable, though the rules connecting the directions of spins with the electric polarization can be modified depending on the symmetry of the bond, which is typically rather low [37,38]. Yet, the magnetoelectric coupling in this case remains antisymmetric with respect to the permutation of e_1 and e_2 . However, if the bonds are noncentrosymmetric, there can be many complications, related to the existence of other contributions to \vec{P} , of isotropic, antisymmetric, and anisotropic symmetric types.

From the viewpoint of symmetry of individual bonds, there are not so many materials where the conventional KNB rule can be realized as it is, without modifications. One of such examples is magnetoelectric Cr_2O_3 [5], those Cr-Cr bonds have threefold rotational symmetry. Nevertheless, another important factor is that, in solid, the behavior of polarization is not necessarily related to the properties of a single bond: there are typically several bonds contributing to \vec{P} , these bonds can have different orientation in space, so that the observable polarization is an averaged property, which can have higher symmetry.

The single-ion anisotropy part of \vec{P} is also subjected to several constraints. It is expected to vanish for the spin $\frac{1}{2}$ and if magnetic ions are located in the inversion centers, which imposes severe restrictions on possible involvement of this mechanism to the behavior of real multiferroic materials. Particularly, considering the properties of proper screw multiferroics, where the conventional KNB mechanism was expected to fail, prompting alternative scenarios based on the single-ion anisotropy [18], most of these magnets appeared to be either spin- $\frac{1}{2}$ or to have magnetic ions in the centrosymmetric positions. Therefore, the single-ion anisotropy mechanism is not applicable. Instead, the properties of proper screw multiferroics can be described by the generalized KNB mechanism, taking into consideration the proper symmetry of magnetic bonds.

Thus, it is already more than twenty years after discovery of multiferroicity—the seemingly exotic phenomenon of breaking the inversion symmetry by a magnetic order and resulting in net electric polarization. The main purpose of this review was to show that, in principle, there is nothing exotic; the magnetic inversion symmetry breaking obey very clear principles, which can be readily established on the phenomenological and microscopical levels. The KNB theory was the first microscopic theory of electric polarization in noncollinear magnets. This theory can be systematically understood and extended on the grounds of modern theory of electric polarization in periodic systems.

Supplementary Materials: The following supporting information can be downloaded at: <https://www.mdpi.com/article/10.3390/condmat10020021/s1>.

Funding: This research received no external funding.

Acknowledgments: I am grateful to Akihiro Tanaka for useful suggestions, help, and constant encouragement in the process of working on this review. MANA is supported by World Premier International Research Center Initiative (WPI), MEXT, Japan.

Conflicts of Interest: The author declares no conflict of interest.

References

1. Lines, M.E.; Glass, A.M. *Principles and Applications of Ferroelectrics and Related Materials*; Oxford University Press: Oxford, UK, 2004.
2. Bersuker, I.B. On the origin of ferroelectricity in perovskite-type crystals. *Phys. Lett.* **1966**, *20*, 589–590. [[CrossRef](#)]
3. Cohen, R.E. Origin of ferroelectricity in perovskite oxides. *Nature* **1992**, *358*, 136–138. [[CrossRef](#)]
4. Hill, N. Why Are There so Few Magnetic Ferroelectrics? *J. Phys. Chem. B* **2000**, *104*, 6694–6709. [[CrossRef](#)]
5. Dzyaloshinskii, I.E. On the magneto-electrical effect in antiferromagnets. *Zh. Eksp. Teor. Fiz.* **1959**, *37*, 881; *JETP (USSR)* **1960**, *10*, 628.
6. Khomskii, D. Classifying multiferroics: Mechanisms and effects. *Physics* **2009**, *2*, 20. [[CrossRef](#)]
7. Kimura, T.; Goto, T.; Shintani, H.; Ishizaka, K.; Arima, T.; Tokura, Y. Magnetic control of ferroelectric polarization. *Nature* **2003**, *426*, 55–58. [[CrossRef](#)]
8. Cheong, S.-W.; Mostovoy, M. Multiferroics: A magnetic twist for ferroelectricity. *Nat. Mater.* **2007**, *6*, 13–20. [[CrossRef](#)]
9. Eerenstein, W.; Mathur, N.D.; Scott, J.F. Multiferroic and magnetoelectric materials. *Nature* **2006**, *442*, 760–765. [[CrossRef](#)]
10. Tokura, Y. Multiferroics as Quantum Electromagnets. *Science* **2006**, *312*, 1481–1482. [[CrossRef](#)]
11. Tokura, Y.; Seki, S. Multiferroics with Spiral Spin Orders. *Adv. Mater.* **2010**, *22*, 1554–1565. [[CrossRef](#)]
12. Yamaguchi, T.; Tsushima, K. Magnetic Symmetry of Rare-Earth Orthochromites and Orthoferrites. *Phys. Rev. B* **1973**, *8*, 5187. [[CrossRef](#)]
13. King-Smith, R.D.; Vanderbilt, D. Theory of polarization of crystalline solids. *Phys. Rev. B* **1993**, *47*, 1651. [[CrossRef](#)] [[PubMed](#)]
14. Vanderbilt, D.; King-Smith, R.D. Electric polarization as a bulk quantity and its relation to surface charge. *Phys. Rev. B* **1993**, *48*, 4442. [[CrossRef](#)] [[PubMed](#)]
15. Resta, R. Electrical polarization and orbital magnetization: The modern theories. *J. Phys. Condens. Matter* **2010**, *22*, 123201. [[CrossRef](#)]
16. Katsura, H.; Nagaosa, N.; Balatsky, A.V. Spin current and magnetoelectric effect in noncollinear magnets. *Phys. Rev. Lett.* **2005**, *95*, 057205. [[CrossRef](#)]
17. Tokura, Y.; Seki, S.; Nagaosa, N. Multiferroics of spin origin. *Rep. Prog. Phys.* **2014**, *77*, 076501. [[CrossRef](#)]
18. Arima, T. Ferroelectricity Induced by Proper-Screw Type Magnetic Order. *J. Phys. Soc. Jpn.* **2007**, *76*, 073702. [[CrossRef](#)]
19. Kurumaji, T.; Seki, S.; Ishiwata, S.; Murakawa, H.; Tokunaga, Y.; Kaneko, Y.; Tokura, Y. Magnetic-Field Induced Competition of Two Multiferroic Orders in a Triangular-Lattice Helimagnet MnI₂. *Phys. Rev. Lett.* **2011**, *106*, 167206. [[CrossRef](#)]
20. Kenzelmann, M.; Lawes, G.; Harris, A.B.; Gasparovic, G.; Broholm, C.; Ramirez, A.P.; Jorge, G.A.; Jaime, M.; Park, S.; Huang, Q.; et al. Direct Transition from a Disordered to a Multiferroic Phase on a Triangular Lattice. *Phys. Rev. Lett.* **2007**, *98*, 267205. [[CrossRef](#)]
21. Dzyaloshinsky, I. A thermodynamic theory of “weak” ferromagnetism of antiferromagnetics. *J. Chem. Phys. Solids* **1958**, *4*, 241–255. [[CrossRef](#)]
22. Moriya, T. Anisotropic Superexchange Interaction and Weak Ferromagnetism. *Phys. Rev.* **1960**, *120*, 91. [[CrossRef](#)]
23. Ono, R.; Nikolaev, S.; Solovyev, I. Fingerprints of spin-current physics on magnetoelectric response in the spin- $\frac{1}{2}$ magnet Ba₂CuGe₂O₇. *Phys. Rev. B* **2020**, *102*, 064422. [[CrossRef](#)]
24. Solovyev, I.V. Superexchange theory of electronic polarization driven by relativistic spin-orbit interaction at half filling. *Phys. Rev. B* **2017**, *95*, 214406. [[CrossRef](#)]
25. Solovyev, I.V. Magnetization-induced local electric dipoles and multiferroic properties of Ba₂CoGe₂O₇. *Phys. Rev. B* **2015**, *91*, 224423. [[CrossRef](#)]
26. Solovyev, I.; Ono, R.; Nikolaev, S. Magnetically Induced Polarization in Centrosymmetric Bonds. *Phys. Rev. Lett.* **2021**, *127*, 187601. [[CrossRef](#)]
27. Anderson, P.W. New Approach to the Theory of Superexchange Interactions. *Phys. Rev.* **1959**, *115*, 2. [[CrossRef](#)]
28. Kugel, K.I.; Khomskii, D.I. The Jahn-Teller effect and magnetism: Transition metal compounds. *Sov. Phys. Usp.* **1982**, *25*, 231. [[CrossRef](#)]
29. Anderson, P.W. Antiferromagnetism. Theory of Superexchange Interaction. *Phys. Rev.* **1950**, *79*, 350. [[CrossRef](#)]
30. Goodenough, J.B. Theory of the Role of Covalence in the Perovskite-Type Manganites [La_{1-x}Sr_xCoO_{3-λ}]. *Phys. Rev.* **1955**, *100*, 564. [[CrossRef](#)]
31. Goodenough, J.B. An interpretation of the magnetic properties of the perovskite-type mixed crystals La_{1-x}Sr_xCoO_{3-λ}. *J. Phys. Chem. Solids* **1958**, *6*, 287–297. [[CrossRef](#)]
32. Kanamori, J. Superexchange interaction and symmetry properties of electron orbitals. *J. Phys. Chem. Solids* **1959**, *10*, 87–98. [[CrossRef](#)]
33. Solovyev, I.V.; Ono, R.; Nikolaev, S.A. Ferromagnetic ferroelectricity due to the Kugel-Khomskii mechanism of orbital ordering assisted by atomic Hund’s second rule effects. *Phys. Rev. B* **2024**, *110*, 205116. [[CrossRef](#)]
34. Yosida, K. *Theory of Magnetism*; Springer: Berlin, Germany, 1998.

35. Murakawa, H.; Onose, Y.; Miyahara, S.; Furukawa, N.; Tokura, Y. Ferroelectricity Induced by Spin-Dependent Metal-Ligand Hybridization in Ba₂CoGe₂O₇. *Phys. Rev. Lett.* **2010**, *105*, 137202. [[CrossRef](#)] [[PubMed](#)]
36. Landau, L.D.; Lifshitz, E.M. *Quantum Mechanics. Non-Relativistic Theory*; Science: Moscow, Russia, 1974.
37. Xiang, H.J.; Kan, E.J.; Zhang, Y.; Whangbo, M.-H.; Gong, X.G. General Theory for the Ferroelectric Polarization Induced by Spin-Spiral Order. *Phys. Rev. Lett.* **2011**, *107*, 157202. [[CrossRef](#)]
38. Kaplan, T.A.; Mahanti, S.D. Canted-spin-caused electric dipoles: A local symmetry theory. *Phys. Rev. B* **2011**, *83*, 174432. [[CrossRef](#)]
39. Solovyev, I.V.; Mazurenko, V.V.; Katanin, A.A. Validity and limitations of the superexchange model for the magnetic properties of Sr₂IrO₄ and Ba₂IrO₄ mediated by the strong spin-orbit coupling. *Phys. Rev. B* **2015**, *92*, 235109. [[CrossRef](#)]
40. Nikolaev, S.A.; Solovyev, I.V. Microscopic theory of electric polarization induced by skyrmionic order in GaV₄S₈. *Phys. Rev. B* **2019**, *99*, 100401(R). [[CrossRef](#)]
41. Astrov, D.N. Magnetolectric effect in chromium oxide. *Zh. Eksp. Teor. Fiz.* **1961**, *40*, 1035; *JETP (USSR)* **1961**, *13*, 729.
42. Solovyev, I.V. Spin-spiral inhomogeneity as the origin of ferroelectric activity in orthorhombic manganites. *Phys. Rev. B* **2011**, *83*, 054404. [[CrossRef](#)]
43. de Gennes, P.-G. Effects of Double Exchange in Magnetic Crystals. *Phys. Rev.* **1960**, *118*, 141. [[CrossRef](#)]
44. Solovyev, I.V.; Nikolaev, S.A. Spin dependence of ferroelectric polarization in the double exchange model for manganites. *Phys. Rev. B* **2014**, *90*, 184425. [[CrossRef](#)]
45. Muñoz, A.; Casáis, M.T.; Alonso, J.A.; Martínez-Lope, M.J.; Martínez, J.L.; Fernández-Díaz, M.T. Complex Magnetism and Magnetic Structures of the Metastable HoMnO₃ Perovskite. *Inorg. Chem.* **2001**, *40*, 1020–1028. [[CrossRef](#)]
46. Okuyama, D.; Ishiwata, S.; Takahashi, Y.; Yamauchi, K.; Picozzi, S.; Sugimoto, K.; Sakai, H.; Takata, M.; Shimano, R.; Taguchi, Y.; et al. Magnetically driven ferroelectric atomic displacements in orthorhombic YMnO₃. *Phys. Rev. B* **2011**, *84*, 054440. [[CrossRef](#)]
47. Solovyev, I.V.; Valentyuk, M.V.; Mazurenko, V.V. Magnetic structure and ferroelectric activity in orthorhombic YMnO₃: Relative roles of magnetic symmetry breaking and atomic displacements. *Phys. Rev. B* **2012**, *86*, 144406. [[CrossRef](#)]
48. Sergienko, I.A.; Dagotto, E. Role of the Dzyaloshinskii-Moriya interaction in multiferroic perovskites. *Phys. Rev. B* **2006**, *73*, 094434. [[CrossRef](#)]
49. Malashevich, A.; Vanderbilt, D. First Principles Study of Improper Ferroelectricity in TbMnO₃. *Phys. Rev. Lett.* **2008**, *101*, 037210. [[CrossRef](#)]
50. Lawes, G.; Harris, A.B.; Kimura, T.; Rogado, N.; Cava, R.J.; Aharony, A.; Entin-Wohlman, O.; Yildirim, T.; Kenzelmann, M.; Broholm, C.; et al. Magnetically driven ferroelectric order in Ni₃V₂O₈. *Phys. Rev. Lett.* **2005**, *95*, 087205. [[CrossRef](#)]
51. Daoud-Aladine, A.; Kundys, B.; Martin, C.; Radaelli, P.G.; Brown, P.J.; Simon, C.; Chapon, L.C. Multiferroicity and spiral magnetism in FeVO₄ with quenched Fe orbital moments. *Phys. Rev. B* **2009**, *80*, 220402. [[CrossRef](#)]
52. Taniguchi, K.; Abe, N.; Takenobu, T.; Iwasa, Y.; Arima, T. Ferroelectric polarization flop in a frustrated magnet MnWO₄ induced by a magnetic field. *Phys. Rev. Lett.* **2006**, *97*, 097203. [[CrossRef](#)]
53. Arkenbout, A.H.; Palstra, T.T.M.; Siegrist, T.; Kimura, T. Ferroelectricity in the cycloidal spiral magnetic phase of MnWO₄. *Phys. Rev. B* **2006**, *74*, 184431. [[CrossRef](#)]
54. Heyer, O.; Hollmann, N.; Klassen, I.; Jodlauk, S.; Bohatý, L.; Becker, P.; Mydosh, J.A.; Lorenz, T.; Khomskii, D. A new multiferroic material: MnWO₄. *J. Phys. Condens. Matter* **2006**, *18*, L471. [[CrossRef](#)]
55. Solovyev, I.V. Origin of multiferroicity in MnWO₄. *Phys. Rev. B* **2013**, *87*, 144403. [[CrossRef](#)]
56. Seki, S.; Kurumaji, T.; Ishiwata, S.; Matsui, H.; Murakawa, H.; Tokunaga, Y.; Kaneko, Y.; Hasegawa, T.; Tokura, Y. Cupric chloride CuCl₂ as an $S = \frac{1}{2}$ chain multiferroic. *Phys. Rev. B* **2010**, *82*, 064424. [[CrossRef](#)]
57. Zhao, L.; Hung, T.-L.; Li, C.-C.; Chen, Y.-Y.; Wu, M.-K.; Kremer, R.K.; Banks, M.G.; Simon, A.; Whangbo, M.-H.; Lee, C.; et al. CuBr₂—A new multiferroic material with high critical temperature. *Adv. Mater.* **2012**, *24*, 2469–2473. [[CrossRef](#)]
58. Kimura, T.; Sekio, Y.; Nakamura, H.; Siegrist, T.; Ramirez, A.P. Cupric oxide as an induced-multiferroic with high-T_C. *Nat. Mater.* **2008**, *7*, 291–294. [[CrossRef](#)]
59. Terada, N.; Khalyavin, D.D.; Manuel, P.; Orlandi, F.; Ridley, C.J.; Bull, C.L.; Ono, R.; Solovyev, I.; Naka, T.; Prabhakaran, D.; et al. Room-temperature type-II multiferroic phase induced by pressure in cupric oxide. *Phys. Rev. Lett.* **2022**, *129*, 217601. [[CrossRef](#)]
60. Rocquefelte, X.; Schwarz, K.; Blaha, P.; Kumar, S.; van den Brink, J. Room-temperature spin-spiral multiferroicity in high-pressure cupric oxide. *Nat. Commun.* **2013**, *4*, 2511. [[CrossRef](#)]
61. Hutanu, V.; Sazonov, A.; Murakawa, H.; Tokura, Y.; Náfrádi, B.; Chernyshov, D. Symmetry and structure of multiferroic Ba₂CoGe₂O₇. *Phys. Rev. B* **2011**, *84*, 212101. [[CrossRef](#)]
62. Zheludev, A.; Shirane, G.; Sasago, Y.; Koide, N.; Uchinokura, K. Spiral phase and spin waves in the quasi-two-dimensional antiferromagnet Ba₂CuGe₂O₇. *Phys. Rev. B* **1996**, *54*, 11879. [[CrossRef](#)]
63. Bogdanov, A.N.; Rößler, U.K.; Wolf, M.; Müller, K.-H. Magnetic structures and reorientation transitions in noncentrosymmetric uniaxial antiferromagnets. *Phys. Rev. B* **2002**, *66*, 214410. [[CrossRef](#)]
64. Skomski, R. *Simple Models of Magnetism*; Oxford University Press: Oxford, UK, 2008.

65. Yildirim, T.; Harris, A.B.; Aharony, A.; Entin-Wohlman, O. Anisotropic spin Hamiltonians due to spin-orbit and Coulomb exchange interactions. *Phys. Rev. B* **1995**, *52*, 10239. [[CrossRef](#)] [[PubMed](#)]
66. Picozzi, S.; Yamauchi, K.; Sanyal, B.; Sergienko, I.A.; Dagotto, E. Dual nature of improper ferroelectricity in a magnetoelectric multiferroic. *Phys. Rev. Lett.* **2007**, *99*, 227201. [[CrossRef](#)] [[PubMed](#)]
67. Solovyev, I.V.; Nikolaev, S.A.; Tanaka, A. Altermagnetism and weak ferromagnetism. *arXiv* **2025**, arXiv:2503.23735.
68. Turov, E.A. *Kinetic, Optical, and Acoustic Properties of Antiferromagnets*; Ural Division of Academy of Sciences of the USSR: Sverdlovsk, Russia, 1990.
69. Turov, E.A. Can the magnetoelectric effect coexist with weak piezomagnetism and ferromagnetism? *Uspekhi Fiz. Nauk* **1994**, *164*, 325; *Physics-Uspekhi* **1994**, *37*, 303–310. [[CrossRef](#)]
70. Tokunaga, Y.; Furukawa, N.; Sakai, H.; Taguchi, Y.; Arima, T.; Tokura, Y. Composite domain walls in a multiferroic perovskite ferrite. *Nat. Mater.* **2009**, *8*, 558–562. [[CrossRef](#)]

Disclaimer/Publisher's Note: The statements, opinions and data contained in all publications are solely those of the individual author(s) and contributor(s) and not of MDPI and/or the editor(s). MDPI and/or the editor(s) disclaim responsibility for any injury to people or property resulting from any ideas, methods, instructions or products referred to in the content.